MATERIALS AND METHODS

Subjects

In total, 91 temporal bones from a collection of 1,278 specimens held at the Department of Otolaryngology, Fukushima Medical University, Japan, were selected for morphometric analyses. We used unilateral temporal bones from 91 different patients. We excluded subjects with history of ear diseases or ototoxic drug use by reviewing their medical records. Pure-tone audiometry had been performed within 24 months of death for all of the selected subjects. Individuals with audiograms showing a characteristic 4,000 Hz dip (that is, thresholds greater than 25 dB at 2 and 8 kHz), which indicates noise-induced HL, were excluded from the study. The subjects ranged in age from 10 to 85 years, with a mean and standard deviation of 59.7 and 16.8 years, respectively.

For all of the chosen subjects, the temporal bones had been removed within 48 hours of death and were fixed with 10% formalin. After decalcification, the temporal bones were embedded in celloidin and serially sectioned in a horizontal plane at a thickness of 20 μm. Every 10th section was stained with hematoxylin-eosin. The adjacent two mid-modiolus sections were subjected to morphometric assessments. In all the specimens used in this study, we found no postmortem degeneration in the SG and SV.

Audiometric Classification

The audiometric hearing-loss patterns were determined based on the air-conductance thresholds at frequencies of 250, 500, 1,000, 2,000, 4,000, and 8,000 Hz. All audiometric patterns with a threshold less than 25 dB were considered to be normal. A flat pattern was defined as HL with a threshold greater than 25 dB and a maximum threshold difference of 20 dB between frequencies of 250 and 8,000 Hz. A high–tone-loss pattern was defined as HL with a threshold greater than 25 dB at 4,000 and 8,000 Hz and a difference in thresholds between 2,000 and 4,000 Hz with an increase of more than 20 dB. A descending pattern was defined as HL with a threshold greater than 25 dB at 2,000, 4,000, and 8,000 Hz and a difference in thresholds between 2,000 and 4,000 Hz with an increase of less than 20 dB. In addition to the audiometric hearing-loss patterns, the average bone-conductance thresholds were determined at the following five frequencies: 250, 500, 1,000, 2,000, and 4,000 Hz. This measure was used as an audiometric parameter.

Morphometric Assessments

Morphometric assessments of the SV and the SG were performed for each cochlear turn at the mid-modiolar level. Images were acquired with a charged-coupling device camera connected to a personal computer. The areas of the SV, Rosenthal's canal, and cochlear turn were quantified by measuring their cut surfaces using Image/J software (http://www.nist.gov/lispix/imlab/prelim/dnld.html) (Fig. 1A). The total number of nuclei in Rosenthal's canal was counted for each cochlear turn. The ratio of the SV area (SV ratio) and the cell density of the SG (SG density) were used to reduce the variance caused by differences in cutting directions among the cochlear specimens. The SV ratio was determined by dividing the SV area by that of the cochlear turn. The SG density was determined by dividing the number of nuclei in Rosenthal's canal by its area.

Statistics

The Pearson's correlation coefficient with Fisher's z transformation was used to examine the relationships between the following variables: age and average bone-conductance threshold; age and SV ratio or SG density for each cochlear turn; and average bone-conductance threshold and SV ratio or SG density. Differences in the SV ratio and SG density according to audiometric pattern were examined by a single factorial analysis of variance. A P value less than .05 was considered statistically significant.

RESULTS

Figure 2 shows the distribution of average bone-conductance thresholds according to age. A significant correlation was discovered between age and average auditory threshold (Fig. 2) ($r = 0.47$, $P < .0001$). This indicated that aging had a significant effect on the elevation of auditory thresholds among the members of the study group.

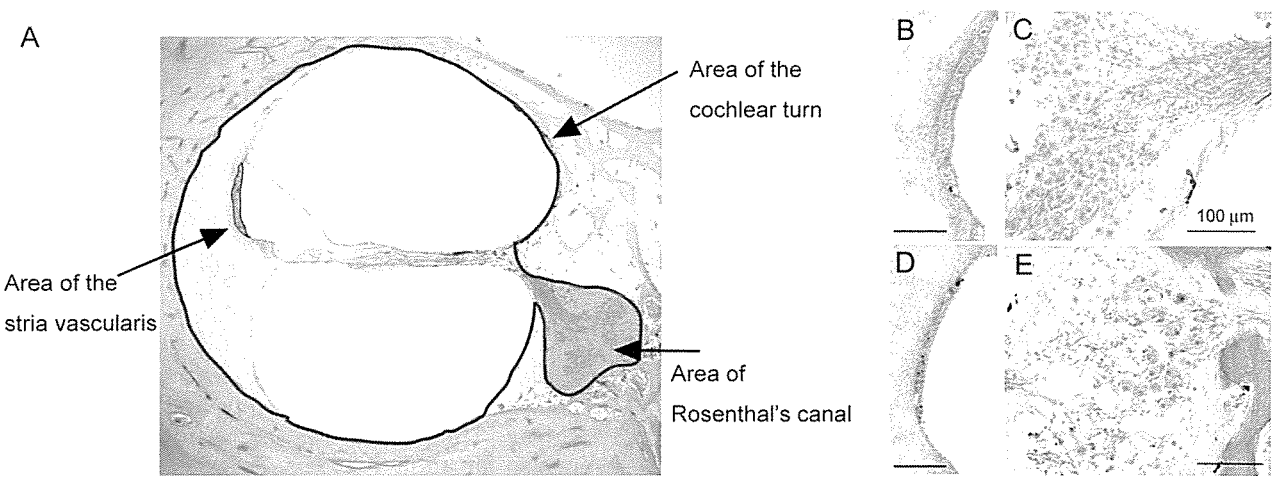

Fig. 1. Morphology of human cochleae. (A) Basal turn of cochlea of 38-year-old male. Area of cochlear turn (black line). Area of SV (dotted line). Area of Rosenthal's canal (gray section). (B) Stria vascularis (SV) of 19-year-old male showing no atrophic changes. (C) Spiral ganglion (SG) of a 37-year-old female exhibiting numerous neurons. (D) SV of 79-year-old male, which is more atrophic than that shown in B. (E) SG of a 77-year-old female, which shows relatively few neurons. Scale bars = 100 μm.

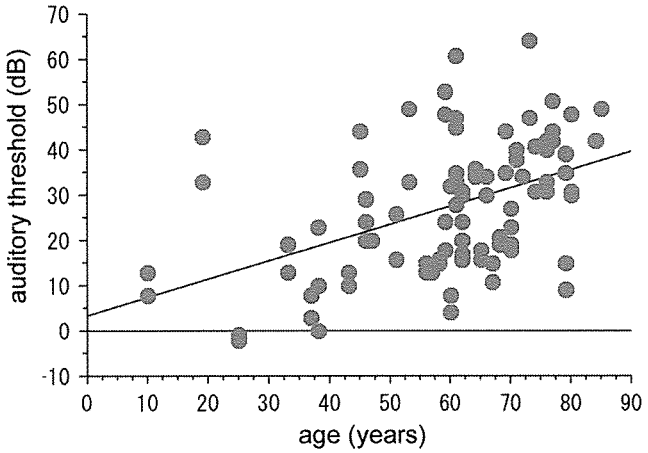

Fig. 2. Relationship between auditory threshold and age. x-axis shows age (years) and y-axis shows average bone-conductance thresholds (dB) at five frequencies (250, 500, 1,000, 2,000, and 4,000 Hz). Significant correlation was detected between average auditory threshold and age using the Pearson's correlation coefficient with Fisher's z transformation ($r = 0.47$, $P < .0001$).

Figure 3 shows the distribution of SV ratios for each cochlear turn according to age. A trend for the SV ratio to decrease with age was seen at every cochlear turn. A significant correlation between age and the SV ratio was found in the basal cochlear turn (Fig. 3A) ($r = -0.36$, $P = .0003$) and the apical cochlear turn (Fig. 3C) ($r = -0.23$, $P = .025$). By contrast, no significant correlation was observed in the middle cochlear turn (Fig. 3B). Figure 4 shows the distribution of SG densities for each cochlear turn according to age. Although the SG densities tended to decrease with age, none of the cochlear turns showed a statistically significant correlation between these variables.

The subjects of the present study were divided into four groups according to their audiometric patterns, as follows: 37 subjects showed a normal pattern, 25 subjects showed a descending pattern, 19 subjects showed a flat pattern, and 10 patients showed a high–tone-loss pattern. The means and standard errors of the SV ratios and SG densities for each audiometric-pattern group are shown in Figure 5. There were no significant differences in either the SV ratios or the SG densities among the audiometric pattern groups for each cochlear turn. We also examined the relationship between the average auditory threshold and the SV ratio or the SG density at each cochlear turn. No significant correlations were observed between these parameters.

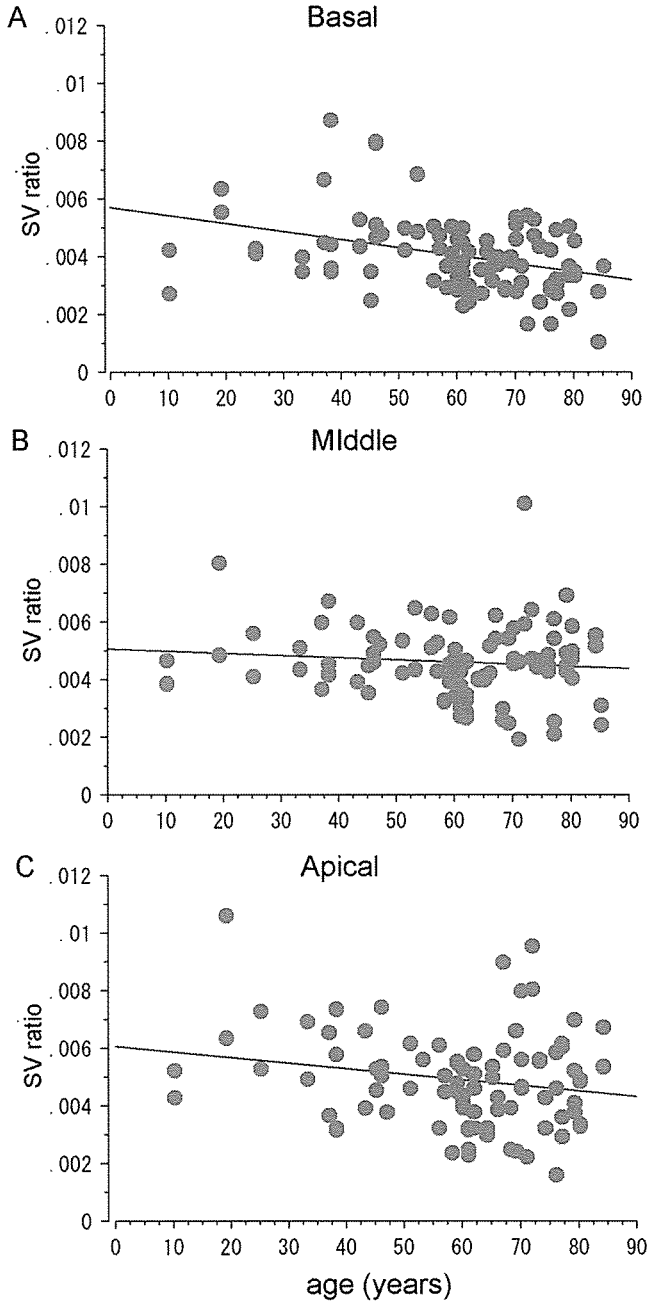

Fig. 3. Relationship between stria vascularis (SV) ratio and age in basal (A), middle (B), and apical (C) cochlear turns. x-axis shows age (yr) and y-axis shows SV ratio. Significant correlations between SV ratio and age were observed in basal and apical cochlear turns according to Pearson's correlation coefficient with Fisher's z transformation ($r = -0.36$, $P = .0003$ and $r = -0.23$, $P = .025$, respectively).

DISCUSSION

The study group in the present analysis was screened to exclude individuals with hearing impairments caused by ototoxic pathogens other than aging by reviewing their medical records and pure-tone audiograms. Morphometric analysis of the 91 selected subjects revealed a significant correlation between auditory threshold and age, which indicated that aging had important effects on hearing performance, at least within our study population.

Our present findings demonstrated a significant correlation between SV atrophy and aging in human cochleae. This was consistent with previous findings reported for animal models. A series of studies on gerbils that were maintained under quiet conditions indicated that SV degeneration was the most prominent age-related histologic change in their cochleae.[6–8] Age-related SV degeneration in these gerbil models was

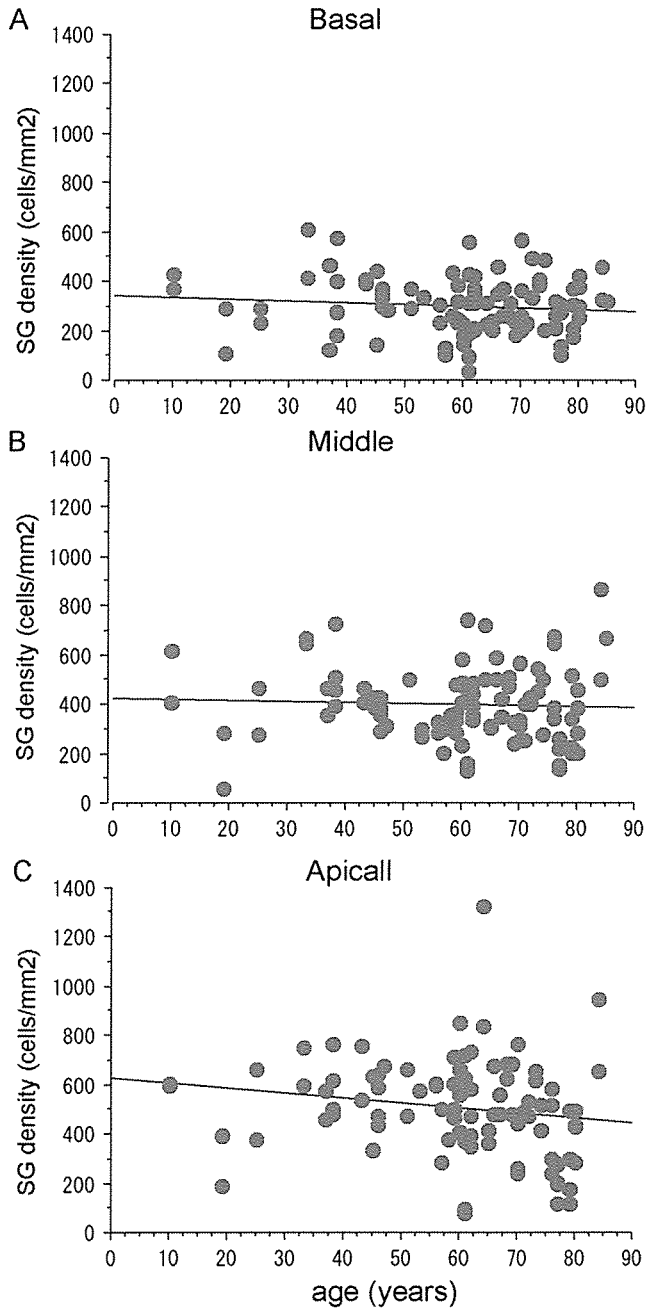

Fig. 4. Relationship between spiral ganglion (SG) density and age in basal (A), middle (B), and apical (C) cochlear turns. x-axis shows age (yr) and y-axis shows SG density. No significant correlations were observed between SG density and age in basal, middle, and apical cochlear turns.

usually found to originate in both the base and the apex of the cochleae. Our present results also identified significant aging effects on SV atrophy in the basal and apical portions of human cochleae. These findings support the hypothesis that SV degeneration is a morphologic characteristic of age-induced cochlear degeneration.

Schuknecht and Gacek[14] described degeneration of the SV as the most prominent morphologic characteristic of age-related HL based on their observations of human temporal bones. Recent morphometric analysis of human temporal bones[20] also supported this hypothesis. Nelson and Hinojosa[19] controversially concluded that SV atrophy was not specific to aged human cochleae with flat audiometric patterns of HL based on a precise morphometric analysis. The present study found no significant correlation between SV atrophy and audiometric patterns of HL or thresholds, although a significant correlation was detected between SV atrophy and aging. Previous studies on human subjects have indicated a poor correlation between audiometric patterns of HL and cochlear histopathology.[15–18] We therefore conclude that SV atrophy is an anatomic characteristic of age-induced cochlear changes but suggest that it is difficult to discern cochlear histopathology from conventional pure-tone audiometry.

The present study failed to find an age-dependent decrease in SG density. By contrast, several previous studies found significant correlations between aging and loss of SG neurons in both humans[15,20] and animal models.[11,12] These reports frequently noted a loss of SG neurons coupled with a loss of cochlear hair cells. Gates and Mills[18] showed that subjects experiencing loss of cochlear hair cells and SG neurons frequently had histories of noise exposure, indicating that these morphologic findings in human cochleae might have been induced by environmental noise. By contrast, in gerbils maintained under quiet conditions, which demonstrated age-dependent SV degeneration, loss of auditory nerve function was indicated by elevation of the compound action potentials of auditory nerves.[10] Recently, changes of the expression patterns of brain-derived neurotrophic factors have been demonstrated in the SG neurons of aged rats and gerbils.[21] This functional degeneration involved no significant loss of SG neurons. We therefore consider that the degeneration of SG neurons might be involved in age-related HL. However, these degenerative changes of the SG neurons cannot be detected by conventional histopathology of human temporal bones.

The present study failed to identify significant correlations between morphologic and audiometric findings in human subjects similar to those reported previously. One possible explanation for this discrepancy is that histologic findings obtained by conventional light microscopy cannot reveal changes in the functionality of cochlear elements, which might play critical roles in the process of age-induced HL.

CONCLUSION

Our present analysis of 91 temporal bones indicates that SV atrophy is the most common histopathologic feature of aged human cochleae. This conclusion is supported by previous observations of aged animal models and human temporal bones. By contrast, age-dependent SG atrophy was not detected by conventional light microscopy in the present study, although several previous studies have indicated a correlation between functional degeneration of SG neurons and aging.

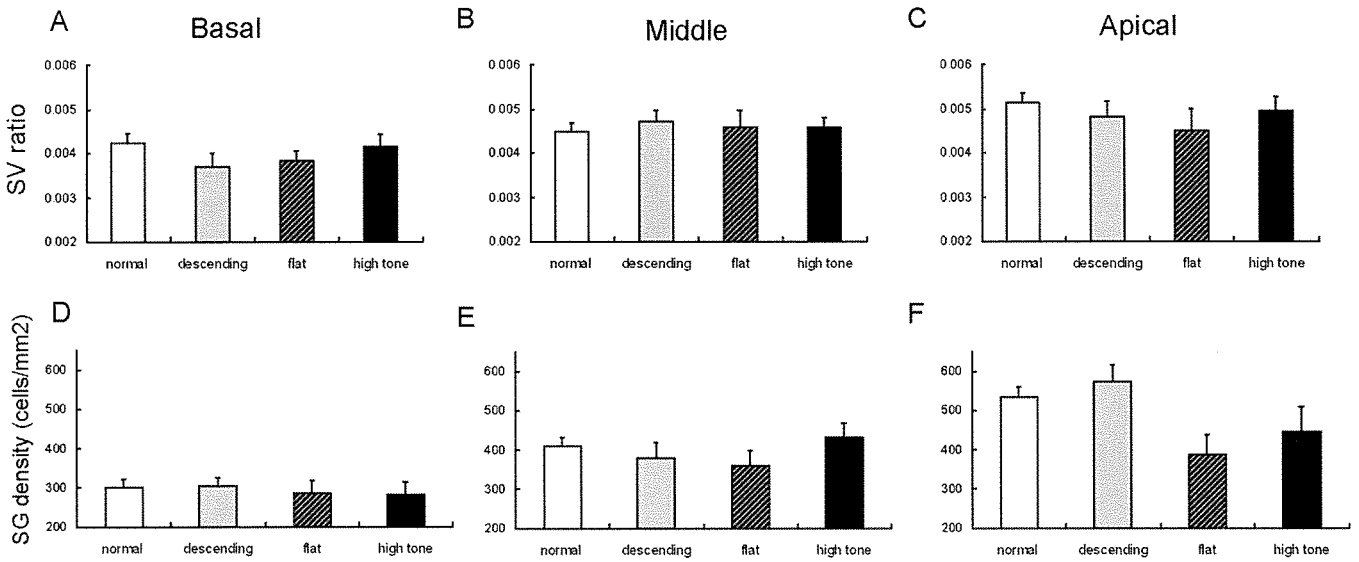

Fig. 5. Means and standard errors of stria vascularis (SV) ratios (A to C) and spiral ganglion (SG) densities (D to F) of experimental groups divided according to audiometric hearing-loss patterns. No significant differences in SV ratios or SG densities were found among experimental groups in the basal, middle, or apical cochlear turns.

Acknowledgments

The authors thank Professor emeritus Iwao Ohtani for his establishment of temporal bone laboratory and Etsuko Sato for her technical contribution to this work.

BIBLIOGRAPHY

1. Izumikawa M, Minoda R, Kawamoto K, et al. Auditory hair cell replacement and hearing improvement by *Atoh1* gene therapy in deaf mammals. *Nat Med* 2005;11:271–276.
2. Okano T, Nakagawa T, Endo T, et al. Engraftment of embryonic stem cell-derived neurons into the cochlear modiolus. *Neuroreport* 2005;16:1919–1922.
3. Seidman MD. Effects of dietary restriction and antioxidants on presbycusis. *Laryngoscope* 2000;110:727–738.
4. Ernfors P, Duan ML, El Shamy WM, Canlon B. Protection of auditory neurons from aminoglycoside toxicity by neurotrophin-3. *Nat Med* 1996;2:463–467.
5. Iwai K, Nakagawa T, Endo T, et al. Cochlear protection by local IGF-1 application using biodegradable hydrogel. *Laryngoscope* 2006;116:526–533.
6. Spicer SS, Schulte BA. Spiral ligament pathology in quiet-aged gerbils. *Hear Res* 2002;172:172–185.
7. Spiess AC, Lang H, Schulte BA, et al. Effects of gap junction uncoupling in the gerbil cochlea. *Laryngoscope* 2002;112: 1635–1641.
8. Schulte BA, Schmiedt RA. Lateral wall Na, K-ATPase and endocochlear potentials decline with age in quiet-reared gerbils. *Hear Res* 1992;61:35–46.
9. Schmiedt RA, Lang H, Okamura HO, Schulte BA. Effects of furosemide applied chronically to the round window: a model of metabolic presbycusis. *J Neurosci* 2002;22: 9643–9650.
10. Hellstrom LI, Schmiedt RA. Compound action potential input/output functions in young and quiet-aged gerbils. *Hear Res* 1990;50:163–174.
11. Shiga A, Nakagawa T, Nakayama M, et al. Aging effects on vestibulo-ocular responses in C57B/6 mice: comparison with alteration in auditory function. *Audiol Neurootol* 2005;10:97–104.
12. Keithley EM, Ryan AF, Woolf NK. Spiral ganglion cell density in young and old gerbils. *Hear Res* 1989;38:125–133.
13. Schuknecht HF. *Pathology of the Ear.* Cambridge, MA: Harvard University Press, 1974.
14. Schuknecht HF, Gacek MR. Cochlear pathology in presbycusis. *Ann Otol Rhinol Laryngol* 1993;102:1–16.
15. Suga F, Lindsay JR. Histopathological observations of presbycusis. *Ann Otol Rhinol Laryngol* 1976;85:169–184.
16. Engstrom B, Hillerdal M, Laurell G, Bagger-Sjöback D. Selected pathological findings in the human cochlea. *Acta Otolaryngol (Stockh)* 1987;436:110–116.
17. Jennings CR, Jones NS. Presbycusis. *J Laryngol Otol* 2001; 115:171–178.
18. Gates GA, Mills JH. Presbycusis. *Lancet* 2005;366:1111–1120.
19. Nelson EG, Hinojosa R. Presbycusis: a human temporal bone study of individuals with flat audiometric patterns of hearing loss using a new method to quantify stria vascularis volume. *Laryngoscope* 2003;113:1672–1686.
20. Kusunoki T, Cureoglu S, Schachern PA, et al. Age-related histopathologic changes in the human cochlea: a temporal bone study. *Otolaryngol Head Neck Surg* 2004;131: 897–903.
21. Rüttiger L, Panford-Walsh R, Schimmang T, et al. BDNF mRNA expression and protein localization are changed in age related hearing loss. *Neurobiol Aging* 2006 March 29; Epub ahead of print.

ARTICLE

doi:10.1016/j.ymthe.2006.06.012

Cell–Gene Delivery of Brain-Derived Neurotrophic Factor to the Mouse Inner Ear

Takayuki Okano, Takayuki Nakagawa,* Tomoko Kita, Tsuyoshi Endo, and Juichi Ito

Department of Otolaryngology–Head and Neck Surgery, Graduate School of Medicine, Kyoto University, 606-8507 Kyoto, Japan

**To whom correspondence and reprint requests should be addressed at the Department of Otolaryngology–Head and Neck Surgery, Graduate School of Medicine, Kyoto University, Kawaharacho 54, Shogoin, Sakyo-ku, 606-8507 Kyoto, Japan. Fax: +81 75 751 7225. E-mail: tnakagawa@ent.kuhp.kyoto-u.ac.jp.*

Available online 7 September 2006

Sensorineural hearing loss is a common disability, but treatment options are currently limited to cochlear implants and hearing aids. Studies are therefore being conducted to provide alternative means of biological therapy, including gene therapy. Safe and effective methods of gene delivery to the cochlea need to be developed to facilitate the clinical application of these therapeutic treatments for hearing loss. In this study, we examined the potential of cell–gene therapy with nonviral vectors for delivery of therapeutic molecules into the cochlea. NIH3T3 cells were transfected with the brain-derived neurotrophic factor (*Bdnf*) gene using lipofection and then transplanted into the mouse inner ear. Immunohistochemistry and Western blotting demonstrated the survival of grafted cells in the cochlea for up to 4 weeks after transplantation. No significant hearing loss was induced by the transplantation procedure. A Bdnf-specific enzyme-linked immunosorbent assay revealed a significant increase in Bdnf production in the inner ear following transplantation of engineered cells. These findings indicate that cell–gene delivery with nonviral vectors may be applicable for the local, sustained delivery of therapeutic molecules into the cochlea.

Key Words: gene therapy, cell transplantation, hearing loss, cochlea, brain-derived neurotrophic factor, nonviral vector

INTRODUCTION

Sensorineural hearing loss (SNHL) is one of the most common disabilities in industrialized countries. Defects in the auditory hair cells, and in their associated spiral ganglion neurons (SGNs), can lead to hearing loss or deafness. Approximately 50% of SNHL cases have a genetic basis, a significant proportion of which is non-syndromic and usually inherited in an autosomal recessive manner [1]. In the past decade, many genetic mutations that cause deafness have been identified, which may contribute to the biological sources available for therapeutic approaches. Should the restoration of mutated genes in the cochlea by gene manipulation become a reality, gene therapy might be a promising method for treating SNHL of genetic origin.

Protecting auditory hair cells and SGNs from irreversible degeneration is a primary objective as inner ear cells have limited regeneration capacity. With the recent increase in understanding of the role of neurotrophic factors, including brain-derived neurotrophic factor (BDNF), on the maintenance of the mature peripheral auditory systems, there have been numerous attempts to define ways to reduce hair cell and SGN degeneration [2–6]. Since neurotrophins have a short serum half-life of just minutes or hours [7], their sustained local delivery is essential for cochlear protection. Previous studies have used viral vectors, particularly adenoviruses or adeno-associated viruses, to deliver neurotrophins to the cochleae [8–13]. However, despite their high transduction efficiency, high titer, and ease of production, viral vectors involve potential toxicity.

Gene therapy could enable the long-term delivery of several agents into the inner ear. Cell transplantation has been used as a means of delivering peptides or proteins into the central nervous system, demonstrating its use as a delivery vehicle for therapeutic molecules [14–16]. In addition, recent studies have demonstrated successful cell transplantation into the mouse cochlea [17,18]. Therefore, transplantation of cells that have been genetically manipulated *in vitro* using nonviral vectors potentially resolves the problem of viral vector toxicity in cochlear gene therapy.

In this study, we conducted an examination of the efficiency of cell–gene delivery into the cochlea for application of therapeutic molecules to the treatment of SNHL. We chose NIH3T3 cells as a delivery vehicle for the

1525-0016/$30.00

gene. NIH3T3 cells are a well-established fibroblast cell line, so that it is easy to optimize conditions for gene transfer and to select gene-expressing cells *in vitro*. In addition, fibroblasts are available from various human sources, which may be advantage for extending future clinical investigations. We transfected NIH3T3 cells with the *Bdnf* gene using lipofection. We then examined the potential for transplanting transfected NIH3T3 cells into the mouse inner ear.

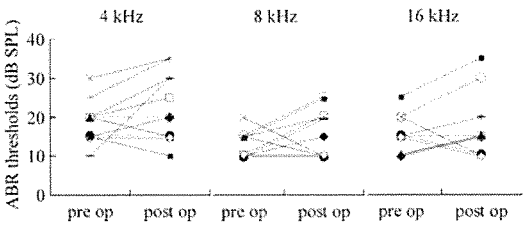

FIG. 1. ABR thresholds before and after cell transplantation. The left lane shows preoperative (pre op) ABR thresholds of each ear, and the right shows those recorded on day 28 after transplantation (post op) at 4, 8, and 16 kHz. The *x* axis shows ABR thresholds (dB SPL).

Results and Discussion

Bdnf Gene Transfer

To determine the efficacy of gene transfection using a nonviral vector, we performed reverse transcriptase-polymerase chain reaction (RT-PCR) analysis of Bdnf mRNA levels in transfected and nontransfected NIH3T3 cells (data not shown). NIH3T3 cells transfected with the mouse *Bdnf* gene (NIH3T3/BDNF) demonstrated Bdnf mRNA expression (86-bp fragment), which was absent from cells transfected with a vector carrying an antibiotic resistance gene (NIH3T3/control) and from nontransfected cells (NIH3T3/original). Amplification of gylceraldehyde-3-phosphate dehydrogenase (*Gapdh*), yielding a 171-bp amplicon, was used as an internal control. Negative control reactions that lacked reverse transcriptase failed to yield amplicons of either *Gapdh* or *Bdnf*.

We carried out an enzyme-linked immunosorbent assay (ELISA) for Bdnf protein to examine the efficacy of Bdnf protein expression and secretion *in vitro*. The mean Bdnf concentration in the culture medium of NIH3T3/BDNF cells, at 396.70 ± 32.66 pg/ml, was significantly higher than in the medium of either NIH3T3/control cells (24.96 ± 5.22 pg/ml) or NIH3T3/original cells (32.42 ± 7.09 pg/ml) ($P < 0.0001$). These findings demonstrate efficient, functional gene transfer into NIH3T3 cells *in vitro* by a liposome-mediated delivery method.

Cell Transplantation into Mouse Cochleae

We transfected NIH3T3 cells with the mouse *Bdnf* gene tagged with a FLAG epitope (NIH3T3/FLAG) to enable transfected, transplanted cells to be readily distinguished from host inner ear cells. We injected suspensions of NIH3T3/FLAG and NIH3T3/control cells into the perilymphatic space of the posterior semicircular canal of C57BL/6 mice using a technique that we developed in previous studies [17,18]. Although delivery of cells into the mouse cochlea is difficult because of its small size, the well-defined genetics of a mouse model enable a variety of analyses of the inner ear to be performed.

We performed auditory brain stem response (ABR) recording to evaluate the effects of the transplantation procedure on hearing (Fig. 1). Alterations in ABR thresholds between pre- and postoperation were limited within 10 dB, although one animal exhibited a 20-dB elevation in ABR thresholds at 4 kHz. Preoperative ABR thresholds were 18.6 ± 1.7 (dB SPL) at 4 kHz, 12.7 ± 1.0 at 8 kHz, and 15.5 ± 1.4 at 16 kHz, and those on postoperative day 28 were 22.7 ± 2.6 at 4 kHz, 15.9 ± 1.9 at 8 kHz, and 17.3 ± 2.5 at 16 kHz. We identified no significant elevation of ABR thresholds on day 28 at frequencies of 4, 8, and 16 kHz. In addition, we observed no vestibular dysfunction in the behavior of the animals after the operation. These findings indicate the limited surgical invasiveness of our transplantation procedure, which is almost identical to previous observations [19,20].

Immunohistochemical analysis of FLAG expression demonstrated the settlement and survival of grafted NIH3T3/FLAG cells in both the cochlea and the vestibule (Figs. 2A, 2B, 2D, 2E). The engrafted cells were clearly distinct from the endogenous cells based on their expression of FLAG, while control specimens that were transplanted with NIH3T3/control cells exhibited no expression of FLAG (Figs. 2C and 2F). Grafted cells were localized in the perilymphatic space of cochleae or vestibules and did not establish in the endolymphatic space or within the inner ear tissues. These locations are identical to those of neural stem cell-derived cells transplanted into the mouse inner ear through the semicircular canal in our previous study [17]. On day 7, we found numerous grafted cells as cell aggregates in the vestibule. On day 28, we still observed grafted cells in both vestibules and cochleae, but did not see aggregation of grafted cells. Of grafted cells located in the perilymphatic space of cochleae, 91.2 ± 11.1% adhered to host cochlear tissues on day 7 and 92.3 ± 14.7% on day 28. The survival and settlement of grafted cells in the inner ear were also demonstrated by Western blotting for FLAG (Fig. 2G). We prepared protein lysates from the inner ear specimens obtained on day 28. The FLAG-tagged *Bdnf* transgene product (31 kDa) was detected in specimens transplanted with NIH3T3/FLAG cells, but not in those transplanted with NIH3T3/control cells. The β-actin internal control was detected in both specimens at equal density. These findings demonstrate that cells transplanted through the posterior semicircular canal survive and produce gene-encoded proteins in the perilymphatic space of cochleae and vestibules, indicating

doi:10.1016/j.ymthe.2006.06.012

FIG. 2. Localization of grafted NIH3T3/FLAG cells in the inner ear and infiltration of CD45-positive cells in cochleae. (A–F) Grafted cells are labeled with FLAG (green fluorescence), and cell nuclei are labeled with DAPI (blue fluorescence). A number of grafted cells are found both in the cochlea (A) and in the vestibule (D) at 1 week after transplantation. In the vestibule, numerous grafted cells form cell aggregates (D). Grafted cells are also identified in the cochlea (B) and vestibule (E) at 4 weeks after transplantation. No FLAG-positive cells were found in the control cochlea (C) or vestibule (F). Bars represent 200 μm and 20 μm in insets. (G) Western blot for FLAG expression in the inner ear at 4 weeks after cell transplantation. The FLAG-tagged Bdnf (31-kDa band) is detected in cochleae engrafted with NIH3T3/BDNF-FLAG cells (lane 1), but not in engrafted control cells (lane 2). β-Actin (42-kDa band), an internal control, is detected in both specimens at the same density. (H–J) Localization of CD45-positive cells in cochleae. In control cochleae, CD45-positive cells (red fluorescence) are found in the spiral ligament and spiral ganglion (arrows in H). CD45-positive cells were localized in the spiral ganglion, osseous spiral lamina, spiral ligament, and spiral limbus (arrows) at 1 (I) and 4 weeks (J) after engraftment of NIH3T3/BDNF-FLAG cells. Blue fluorescence shows DAPI. Bars represent 200 μm.

sustained delivery of Bdnf from transplanted cells to the perilymphatic space of the inner ears. Previous investigations have demonstrated that application of neurotrophins, including Bdnf, into the perilymph efficiently protects hair cells or spiral ganglion neurons from various ototoxic insults [2–6,10,11], indicating that neurotrophins delivered in the perilymph act on hair cells and spiral ganglion neurons. We therefore consider that Bdnf secreted from transplanted cells may be accessible to hair cells and spiral ganglion neurons.

The numbers of FLAG-positive cells in the cochlea decreased from the time point of day 7 to that of day 28. On day 7 after transplantation, we observed 26.7 ± 3.3 grafted cells in one midmodiolus section of cochleae, while we found 14.4 ± 2.3 cells on day 28. We then analyzed infiltration of inflammatory cells into cochlear tissues to investigate immune-mediated clearance of grafted cells. We employed immunohistochemistry for CD45, a leukocyte common antigen, to determine the distribution of inflammatory cells in the cochlea. In control cochleae, we found CD45-positive cells in the spiral ganglion, spiral limbus, and spiral ligament (Fig. 2H). Cochleae that received transplantation of NIH3T3/FLAG cells exhibited a similar distribution of CD45-positive cells compared to that of control cochleae (Figs. 2I and 2J). We observed no obvious infiltration of CD45-positive cells into the perilymphatic space of cochleae. These findings demonstrate that infiltration of inflammatory cells is not induced by transplantation of NIH3T3/FLAG cells into the inner ears. Even after xenografts into the cochlear fluid space without use of immune suppressants, cell infiltration into the cochlear fluid space has not been observed [21]. We therefore consider that immune-mediated clearance may not play a central role in elimination of transplanted cells from the inner ear. However, further studies are required to determine actual roles of the immune system in the decrease in transplanted cells in the inner ears.

Efficiency of Gene Delivery

We performed an ELISA of Bdnf proteins extracted from the inner ear to examine the efficiency of cell–gene delivery. We collected the inner ear specimens on day 7 after transplantation and calculated the ratio of Bdnf concentration to total protein in the sample solutions. NIH3T3/BDNF cell-transplanted specimens showed a significantly higher ratio (93.40 ± 10.69 pg/mg total protein) compared with NIH3T3/control cell-transplanted samples (46.68 ± 4.41 pg/mg) ($P = 0.01$). There was no significant difference between the levels of total protein extracted from the two samples (NIH3T3/BDNF, 2.65 ± 0.21 mg/ml; NIH3T3/control, 2.77 ± 0.12 mg/ml). These findings demonstrate that Bdnf synthesis by engrafted NIH3T3/BDNF cells contributes to a significant increase in Bdnf protein levels of the inner ear specimens, suggesting that cell–gene therapy may be applicable for local, sustained delivery of therapeutic molecules into the inner ear.

This is the first report that demonstrates the successful cell–gene delivery of therapeutic molecules to the cochlea without the use of viral vectors, an encouraging result for the extension of research into gene therapy for the inner ear. Currently, several experiments utilize human fibroblasts as a delivery vehicle [22,23]. The use of autologous bone marrow-derived stromal cells for transplants into the inner ear has been reported [24]. Such cells eliminate the risk of immunoresponses, and their ability to migrate into the cochlear lateral wall and modiolus is likely to enhance the potential for delivery of genes into these areas of the cochlea. Future studies should be performed to evaluate the potential of these alternative transplant media as a vehicle for gene delivery.

In summary, we transplanted NIH3T3 cells that had been genetically engineered to express Bdnf into the mouse inner ear and evaluated the efficiency of transplantation for local delivery of gene products. The results demonstrated a significant increase in Bdnf protein in the inner ear following transplantation of engineered cells. These findings indicate that gene therapy may be a feasible treatment option for inner ear diseases such as SNHL. Cell–gene delivery of therapeutic molecules into the inner ear is suitable for protection of inner ear cells against gradually progressive degeneration. Presbycusis, age-related hearing loss, may be included in targets for cell–gene therapy. BDNF application via cell–gene delivery could be an efficient strategy for promotion of survival of SGNs in cases of cochlear implants (CIs), which are small devices that are surgically implanted in the cochlea to stimulate SGNs. BDNF transgene produced by gene-engineered cells will support the survival of SGNs after CI surgery, which can contribute to the maintenance of hearing benefits provided by CIs.

Materials and Methods

Animals. Forty-three 10-week-old male C57BL/6 mice (SLC Japan, Hamamatsu, Japan) with normal hearing were used in the study. All mice were maintained in the Institute of Laboratory Animals, Kyoto University Graduate School of Medicine. All experimental protocols were approved by the Animal Research Committee, Kyoto University Graduate School of Medicine, and conducted in accordance with NIH guidelines for the care and use of laboratory animals.

Vector construction. The *Mus musculus* (house mouse) brain-derived neurotrophic factor cDNA clone (GenBank Accession No. BC034862) was obtained from Invitrogen (Carlsbad, CA, USA). PCR amplification of the cDNA using Pyrobest DNA polymerase (TaKaRa-Bio, Kyoto, Japan) was performed with the following primer pairs: 5′ primer, 5′-GGAATTCGCCACCATGACCATCCTTTTCCTTACTATGG-3′; 3′ primer 1, 5′-ATAAGAATAAGCGGCCGCTCATCTTCCCCTTTTAATGGTCAGTG-3′; and 3′ primer 2, incorporating two pairs of FLAG epitope, 5′-ATAAGAATAAGCGGCCGCTCACTTGTCATCGTCGTCCTTGTAGTCCTTGTCATCGTCGTCCTTGTAGTCCTTGTCATCGTCGTCCTTGTAGTCTCTTCCCCTTTTAATGGTCAGTG-3′. PCR products were digested with *Eco*RI and *Not*I, and a 0.77-kb

doi:10.1016/j.ymthe.2006.06.012

*Eco*RI–*Not*I fragment containing mouse *Bdnf* or mouse *Bdnf* with FLAG epitope was cloned into the *Eco*RI–*Not*I site of the pIRESneo3 vector (BD Biosciences, Palo Alto, CA, USA) using Ligation Solution (TaKaRa-Bio) to generate plasmid pIRESneo3-bdnf (supplementary information) or pIRESneo3-bdnfflag. For subsequent experiments, plasmid pIRESneo3 containing the neomycin-resistant gene only (pIRESneo3-control) was also amplified. Restriction analysis and DNA sequencing were used to confirm the integrity of all constructs.

Cell lines and gene transfer. NIH3T3 cells were obtained from Riken Cell Bank (RCB 0150; Tsukuba, Japan) and cultured in Dulbecco's modified Eagle's medium (DMEM; GIBCO BRL, Grand Island, NY, USA) containing 10% newborn calf serum (GIBCO), penicillin (100 U/ml), streptomycin (100 μg/ml), and amphotericin B (0.25 μg/ml) in a humidified atmosphere of 5% CO_2 at 37°C. NIH3T3 cells were plated at a density of 1×10^5 cells per 100-mm plastic dish and incubated for 48 h. Transfection was performed with 18 μl of FuGENE6 Transfection Reagent (Roche, Indianapolis, IN, USA) complexed with 9 μg pIRESneo3-bdnf, pIRESneo3-bdnfflag, or pIRESneo3-control plasmid in DMEM per 100-mm plastic dish at 37°C for 6 h. The medium was then replaced with conditioned medium containing Geneticin sulfate (G418; Sigma, St. Louis, MO, USA) for the selection of stably transfected cell clones.

Bdnf mRNA expression in cell lines. The expression of Bdnf mRNA in the cell lines was analyzed with RT-PCR. Total RNA was extracted from the cultured cell lines using the RNeasy Kit (Qiagen GmbH, Germany) and then treated with DNase I (Ambion, Austin, TX, USA). Four sets of total RNA for each cell line were prepared. PCRs were performed using TaqMan Gold PCR Master Mix (Applied Biosystems, Foster City, CA, USA) and Bdnf-specific primers. Gapdh mRNA was used as the invariant control. All reactions were performed in triplicate.

Bdnf secretion from cell lines. Bdnf protein levels in culture medium were measured by ELISA to examine Bdnf secretion by transfected cells. NIH3T3/BDNF, NIH3T3/control, and NIH3T3/original cells (1×10^5) were inoculated in 60-mm plastic dishes with 3 ml conditioned medium. The supernatants of the conditioned media were harvested approximately 24 h after inoculation. ELISA was performed using the BDNF Emax Immunoassay System (Promega, Madison, WI, USA) according to the manufacturer's instructions. Four sets of samples were prepared from each cell line, and all reactions were performed in triplicate.

Cell transplantation. On the day of transplantation, cultured cells were suspended at 3×10^4 cells/μl DMEM/F12 (GIBCO). NIH3T3/BDNF cells were transplanted into 10 animals, NIH3T3/FLAG cells into 24 animals, and NIH3T3/control cells into 9 animals. Cell transplantation was performed under general anesthesia with 75 mg/kg ketamine and 9 mg/kg xylazine. A retroauricular incision was made in the left ear, and the posterior semicircular canal (PSCC) was exposed. A small hole was made in the bony wall of the PSCC. A fused silica glass needle (EiCOM, Kyoto, Japan) was then inserted into the perilymphatic space of the PSCC, and the cell suspension was injected at the rate of 1 μl/min for 3 min using a Micro Syringe Pump (EiCOM).

Measurement of auditory function. The auditory function of experimental animals was monitored by ABR recording. ABR measurements were performed as previously described [25]. ABRs were recorded before cell transplantation and on day 28 in the 11 animals that received an engraftment of NIH3T3/FLAG cells. Thresholds were determined for frequencies of 4, 8, and 16 kHz.

Immunohistochemistry. Under general anesthesia, the animals that had been engrafted with NIH3T3/BDNF-FLAG cells were transcardially perfused with phosphate-buffered saline, pH 7.4, followed by 4% paraformaldehyde in phosphate buffer at pH 7.4 on day 7 ($n=10$) or 28 ($n=10$). Immediately, the temporal bones were dissected out and immersed in the same fixative for 4 h at 4°C. Specimens were prepared as cryostat sections. Two midmodiolus sections were chosen from each specimen and stained by immunohistochemistry for FLAG to distinguish transplanted cells from host specimens. Two cochleae on day 7 after transplantation of NIH3T3/control cells were used as controls for immunostaining for FLAG. We counted the numbers of FLAG-positive cells and those of FLAG-positive cells that adhered to cochlear tissues. The ratios of grafted cell that adhered to cochlear tissues were then calculated. The emergence of CD45-positive cells was also examined to evaluate inflammatory response following cell transplantation. Untreated cochlear specimens were served as controls for immunostaining for CD45. Anti-FLAG M2 mouse monoclonal antibody (1:230; Sigma) or anti-mouse CD45 rat monoclonal antibody (a leukocyte common antigen, Ly-5, 1:20; BD PharMingen, San Diego, CA, USA) was used as the primary antibody, and FITC-conjugated goat anti-mouse antibody (1:500; Santa Cruz Biotechnology, Santa Cruz, CA, USA) or Alexa-Fluor 546-conjugated anti-rat antibody (1:500; Molecular Probes, Eugene, OR, USA) was used as the secondary antibody. Counterstaining by 4′,6-diamidino 2-phenylindole dihydrochloride (DAPI; 1 μg/ml; Molecular Probes) was performed to demonstrate nuclear locations.

FLAG Western blotting. The expression of FLAG-tagged Bdnf fusion protein in the inner ear engrafted with NIH3T3/FLAG cells ($n=4$) or NIH3T3/control cells ($n=4$) was determined by Western blotting 28 days after transplantation. The temporal bones were homogenized in ice-cold lysis buffer. After centrifugation of the homogenized solution, the supernatants were assayed for proteins. The sample solutions were electroblotted onto a polyvinyldifluoride membrane. The primary antibody was a mouse monoclonal anti-FLAG antibody (1:500; Sigma) or rabbit polyclonal anti-β-actin antibody (1:200; Sigma), and the secondary antibody was HRP-conjugated anti-mouse IgG (1:50,000; Amersham Biopharmacia Biotech, Buckinghamshire, UK) or anti-rabbit IgG (1:25,000; Amersham Biopharmacia Biotech). Reactions were visualized by chemiluminescence using an ECL Plus Western blotting reagent pack (Amersham Biopharmacia Biotech).

Measurement of Bdnf levels in the inner ear. To assess the *in vivo* production of Bdnf protein by grafted cells, the inner ears engrafted with NIH3T3/BDNF cells ($n=10$) or NIH3T3/control cells ($n=5$) were removed on day 7 after transplantation. A Bdnf ELISA was performed using the BDNF Emax Immunoassay System (Promega) according to the manufacturer's protocol. All reactions were performed in triplicate. Total protein concentration was measured with the Lowry assay using the Bio-Rad DC Protein Assay (Bio-Rad, Hercules, CA, USA).

Statistical analysis. Results were expressed as means ± standard error. Statistical analyses for Bdnf levels in the cultured medium and ABR threshold shifts were performed using one-way ANOVA followed by Sheffe's multiple-comparison tests. A Mann–Whitney *U* test was used to compare cochlear Bdnf levels. Probability (*P*) values less than 5% were considered significant.

ACKNOWLEDGMENTS

The authors thank Daisuke Yabe and Norio Yamamoto (Department of Medical Chemistry and Molecular Biology, Kyoto University Graduate School of Medicine, Japan) for help and instruction with molecular biology, Junko Okano (Department of Anatomy and Developmental Biology, Kyoto University Graduate School of Medicine) for critical discussion, and Yoko Nishiyama and Rika Sadato for their technical assistance. This study was supported by a Grant-in-Aid for Scientific Research (B2, 16390488, 2004–2006, T.N.) from the Ministry of Education, Culture, Sports, Science, and Technology of Japan and in part by a grant (2005–2006, T.N.) from the Takeda Science Foundation and a grant (2005, T.O.) from the 21st Century COE Program of the Ministry of Education, Culture, Sports, Science, and Technology of Japan.

RECEIVED FOR PUBLICATION MARCH 7, 2006; REVISED JUNE 8, 2006; ACCEPTED JUNE 21, 2006.

APPENDIX A. SUPPLEMENTARY DATA

Supplementary data associated with this article can be found, in the online version, at doi:10.1016/j.ymthe.2006.06.012.

REFERENCES

1. Nance, W. E. (2003). The genetics of deafness. *Ment. Retard. Dev. Disabil. Res. Rev.* **9:** 109–119.
2. Altschuler, R. A., Cho, Y., Ylikoski, J., Pirvola, U., Magal, E., and Miller, J. M. (1999). Rescue and regrowth of sensory nerves following deafferentation by neurotrophic factors. *Ann. N.Y. Acad. Sci.* **884:** 305–311.
3. Gillespie, L. N., Clark, G. M., Bartlett, P. F., and Marzella, P. L. (2003). BDNF-induced survival of auditory neurons in vivo: cessation of treatment leads to accelerated loss of survival effects. *J. Neurosci. Res.* **71:** 785–790.
4. Endo, T., *et al.* (2005). Novel strategy for treatment of inner ears using a biodegradable gel. *Laryngoscope* **115:** 2016–2020.
5. Noushi, F., Richardson, R. T., Hardman, J., Clark, G., and O'Leary, S. (2005). Delivery of neurotrophin-3 to the cochlea using alginate beads. *Otol. Neurotol.* **26:** 528–533.
6. Shinohara, T., *et al.* (2002). Neurotrophic factor intervention restores auditory function in deafened animals. *Proc. Natl. Acad. Sci. USA* **99:** 1657–1660.
7. Kishino, A., *et al.* (2001). Analysis of effects and pharmacokinetics of subcutaneously administered BDNF. *Neuroreport* **12:** 1067–1072.
8. Staecker, H., Gabaizadeh, R., Federoff, H., and Van De Water, T. R. (1998). Brain-derived neurotrophic factor gene therapy prevents spiral ganglion degeneration after hair cell loss. *Otolaryngol. Head Neck Surg.* **119:** 7–13.
9. Chen, X., Frisina, R. D., Bowers, W. J., Frisina, D. R., and Federoff, H. J. (2001). HSV amplicon-mediated neurotrophin-3 expression protects murine spiral ganglion neurons from cisplatin-induced damage. *Mol. Ther.* **3:** 958–963.
10. Yagi, M., Magal, E., Sheng, Z., Ang, K. A., and Raphael, Y. (1999). Hair cell protection from aminoglycoside ototoxicity by adenovirus-mediated overexpression of glial cell line-derived neurotrophic factor. *Hum. Gene Ther.* **10:** 813–823.
11. Hakuba, N., *et al.* (2003). Adenovirus-mediated overexpression of a gene prevents hearing loss and progressive inner hair cell loss after transient cochlear ischemia in gerbils. *Gene Ther.* **10:** 426–433.
12. Nakaizumi, T., Kawamoto, K., Minoda, R., and Raphael, Y. (2004). Adenovirus-mediated expression of brain-derived neurotrophic factor protects spiral ganglion neurons from ototoxic damage. *Audiol. Neurootol.* **9:** 135–143.
13. Stone, I. M., Lurie, D. I., Kelley, M. W., and Poulsen, D. J. (2005). Adeno-associated virus-mediated gene transfer to hair cells and support cells of the murine cochlea. *Mol. Ther.* **11:** 843–848.
14. Cejas, P. J., *et al.* (2000). Lumbar transplant of neurons genetically modified to secrete brain-derived neurotrophic factor attenuates allodynia and hyperalgesia after sciatic nerve constriction. *Pain* **86:** 195–210.
15. Cao, L., *et al.* (2004). Olfactory ensheathing cells genetically modified to secrete GDNF to promote spinal cord repair. *Brain* **127:** 535–549.
16. Girard, C., *et al.* (2005). Grafts of brain-derived neurotrophic factor and neurotrophin 3-transduced primate Schwann cells lead to functional recovery of the demyelinated mouse spinal cord. *J. Neurosci.* **25:** 7924–7933.
17. Iguchi, F., *et al.* (2003). Trophic support of mouse inner ear by neural stem cell transplantation. *Neuroreport* **14:** 77–80.
18. Tateya, I., *et al.* (2003). Fate of neural stem cells grafted into injured inner ears of mice. *Neuroreport* **14:** 1677–1681.
19. Iguchi, F., *et al.* (2004). Surgical techniques for cell transplantation into the mouse cochlea. *Acta Otolaryngol. Suppl.* **551:** 43–47.
20. Kawamoto, K., Oh, S. H., Kanzaki, S., Brown, N., and Raphael, Y. (2001). The functional and structural outcome of inner ear gene transfer via the vestibular and cochlear fluids in mice. *Mol. Ther.* **4:** 575–585.
21. Hildebrand, M. S., *et al.* (2005). Survival of partially differentiated mouse embryonic stem cells in the scala media of the guinea pig cochlea. *J. Assoc. Res. Otolaryngol.* **6:** 341–354.
22. Evans, C. H., *et al.* (2005). Gene transfer to human joints: progress toward a gene therapy of arthritis. *Proc. Natl. Acad. Sci. USA* **102:** 8698–8703.
23. Kakeda, M., *et al.* (2005). Human artificial chromosome (HAC) vector provides long-term therapeutic transgene expression in normal human primary fibroblasts. *Gene Ther.* **12:** 852–856.
24. Naito, Y., *et al.* (2004). Transplantation of bone marrow stromal cells into the cochlea of chinchillas. *Neuroreport* **15:** 1–4.
25. Shiga, A., *et al.* (2005). Aging effects on vestibulo-ocular responses in C57B/6 mice: comparison with alteration in auditory function. *Audiol. Neurootol.* **10:** 97–104.

The Laryngoscope
Lippincott Williams & Wilkins, Inc.

Cochlear Protection by Local Insulin-Like Growth Factor-1 Application Using Biodegradable Hydrogel

Koji Iwai, MD; Takayuki Nakagawa, MD, PhD; Tsuyoshi Endo, MD; Yoshinori Matsuoka; Tomoko Kita, PhD; Tae-Soo Kim, MD, PhD; Yasuhiko Tabata, PhD; Juichi Ito, MD, PhD

Objective: **The aim of this experimental study was to examine the potential of local recombinant human insulin-like growth factor-1 (rhIGF-1) application through a biodegradable hydrogel for the treatment of cochleae.** ***Methods:*** **A hydrogel immersed with rhIGF-1 was placed on the round window membrane of Sprague-Dawley rats while a hydrogel immersed with physiological saline was applied to control animals. On day 3 after drug application, the animals were exposed to white noise at 120 dB sound pressure level (SPL) for 2 hours. Cochlear function was monitored using measurements of auditory brain stem responses (ABRs) at frequencies of 8, 16, and 32 kHz. The temporal bones were collected 7 or 30 days after noise exposure and the loss of hair cells was quantitatively analyzed.** ***Results:*** **Local rhIGF-1 treatment significantly reduced the elevation of ABR thresholds on days 7 and 30 after noise exposure. Histologic analysis revealed that local rhIGF-1 treatment significantly prohibited the loss of outer hair cells.** ***Conclusions:*** **These findings demonstrate that local IGF-1 application through the biodegradable hydrogel has the potential for protection of cochleae from noise trauma.** ***Key Words:*** **Drug delivery, cochlea, hair cell, protection, growth factor, acoustic trauma, rat.**
Laryngoscope, **116:529–533, 2006**

INTRODUCTION

In recent years, there has been increasing interest in the treatment of inner ear disorders using the local, rather than systemic, application of therapeutic agents, because the former has fewer side effects and is more target-specific. The establishment of clinically applicable strategies for the local application of therapeutic agents should therefore open a new window for the treatment of inner ear disorders. For methods of drug delivery to be viable in clinical settings, it is crucial for the procedure to be technically undemanding and as minimally invasive as possible. Based on such a background, the use of biodegradable polymers for cochlear drug delivery has been investigated.[1–3] Biodegradable polymers, which enable the sustained release of drugs to the cochlear fluid space, can be applied through an intratympanic injection. Among biodegradable polymers, we have reported the efficacy of the biodegradable hydrogel, which is made from porcine type-I collagen, for delivery of brain-derived neurotrophic factor (BDNF) into the cochlear fluid and successful protection of spiral ganglion neurons (SGNs) from degeneration as a result of the loss of cochlear hair cells.[3]

Insulin-like growth factor-1 (IGF-1) is a mitogenic peptide that plays essential roles in the regulation of growth and development in various parts of the body, including the inner ear.[4] IGF-1 is also known to be a neuroprotective agent.[5] In addition, previous studies on the inner ear have suggested the possibility of inner ear protection by IGF-1.[6,7] Moreover, recombinant human IGF-1 (rhIGF-1) has already been approved for clinical use. Our ultimate goal is for local neurotrophin application to be clinically approved for the treatment of inner ears. In the present study, we then selected rhIGF-1 as a suitable neurotrophin for local application to the cochlea using a biodegradable hydrogel as a vehicle for drug delivery. We evaluated whether the application of rhIGF-1 in this manner was effective in protecting against noise-induced hearing loss.

From the Department of Otolaryngology–Head and Neck Surgery (K.I., T.N., T.E., Y.M., T.K., T.-S.K., J.I.), Graduate School of Medicine and the Institute for Frontier Medical Science (Y.T.), Kyoto University, Kyoto, Japan.

Editor's Note: This Manuscript was accepted for publication December 5, 2005.

This study was supported by a Grant-in-Aid for Regenerative Medicine Realization from the Ministry of Education, Science, Sports, Culture and Technology of Japan.

Send Correspondence to Dr. Takayuki Nakagawa, Department of Otolaryngology–Head and Neck Surgery, Graduate School of Medicine, Kyoto University, Kawaharacho 54, Shogoin, Sakyo-ku, 606-8507 Kyoto, Japan. E-mail: tnakagawa@ent.kuhp.kyoto-u.ac.jp

DOI: 10.1097/01.mlg.0000200791.77819.eb

MATERIALS AND METHODS

Experimental Animals

Sprague-Dawley rats (Japan SLC Inc., Hamamatsu, Japan) at 10 weeks of age were used as experimental animals. The Animal Research Committee of the Graduate School of Medicine, Kyoto University, Japan, approved all experimental protocols. Animal care was conducted under the supervision of the Institute of Laboratory Animals at the Graduate School of Medicine, Kyoto University. All experimental procedures were performed in accordance with the U.S. National Institutes of Health guidelines for the care and use of laboratory animals.

Preparation of Hydrogels

The biodegradable hydrogels were prepared as described previously.[8] Briefly, the gels were generated by the glutaraldehyde crosslinking of porcine type-I collagen (Gunze, Ayabe, Japan). The rates of degradation were determined according to the concentration of glutaraldehyde. The present study used a hydrogel that was made with 60 mol/L glutaraldehyde, which could release basic fibroblast growth factor[8] and BDNF[3] for 7 days in vivo.

Local Application of Insulin-Like Growth Factor-1

RhIGF-1 was provided by Astellas Pharma Inc., Tokyo, Japan. After measuring the auditory brain stem responses (ABRs), the otic bulla of the left temporal bone was exposed using a retroauricular approach under general anesthesia with ketamine (100 mg/kg intramuscularly [IM]; Sankyo Co., Tokyo, Japan) and xylazine (9 mg/kg IM; Bayer, Tokyo, Japan). A small hole was made on the left bulla to expose the round window niche. A hydrogel in dry condition was cut into the size of 2 mm^3 under the microscope and immersed with rhIGF-1 (400 μg dissolved in 40 μL physiological saline) 30 minutes before application. The hydrogel was then placed on the round window membrane (RWM) of the IGF group animals (n = 10). The animals applied a hydrogel-immersed physiological saline were used as controls (n = 10).

Noise Exposure and Measurement of Hearing

On day 3 after the IGF-1 application, we measured the ABRs to eliminate animals that showed threshold shifts of more than 10 dB at any frequencies from the experiments. In consequence, no animals showed threshold shifts over 10 dB after local drug application in the present study. The animals were then exposed to white noise at 120 dB sound pressure level (SPL) for 2 hours in a ventilated sound exposure chamber. The sound levels were monitored and calibrated at multiple locations within the sound chamber to ensure uniformity of the stimulus.

Auditory function was assessed by recording ABRs. The measurements of ABR thresholds were performed at frequencies of 8, 16, and 32 kHz before noise exposure and days 7 and 30 after noise exposure. Animals were anesthetized with ketamine (100 mg/kg) and xylazine (9 mg/kg) and kept warm with a heating pad. Generation of acoustic stimuli and subsequent recording of evoked potentials were performed using a PowerLab/4sp (AD Instruments, Castle Hill, Australia). Acoustic stimuli, consisting of tone-burst stimuli (0.1 ms cos^2 rise/fall and 1-ms plateau), were delivered monaurally through a speaker (ES1spc; Bioresearch Center, Nagoya, Japan) connected to a funnel fitted into the external auditory meatus. To record bioelectrical potentials, subdermal stainless steel needle electrodes were inserted at the vertex (ground), ventrolateral to the measured ear (active) and contralateral to the measured ear (reference). Stimuli were calibrated against a ¼-inch free-field microphone (ACO-7016; ACO Pacific, Inc., Belmont, CA) connected to an oscilloscope (DS-8812 DS-538; Iwatsu Electric, Tokyo, Japan) or a sound level meter (LA-5111; Ono Sokki, Yokohama, Japan). The responses between the vertex and mastoid subcutaneous electrodes were amplified with a digital amplifier (MA2; Tucker-Davis Technologies, Alachua, FL). Thresholds were determined from a set of responses at varying intensities with 5-dB SPL intervals and electrical signals were averaged for 1024 repetitions. Thresholds at each frequency were verified at least twice.

Histologic Analysis

On day 7 or 30 after noise exposure, five cochleae from each experimental group were provided for histologic analysis. The animals were anesthetized with ketamine and xylazine, and the left cochleae were exposed. After removal of otic vesicles, 4% paraformaldehyde in 0.01 mol/L phosphate-buffered saline (PBS)

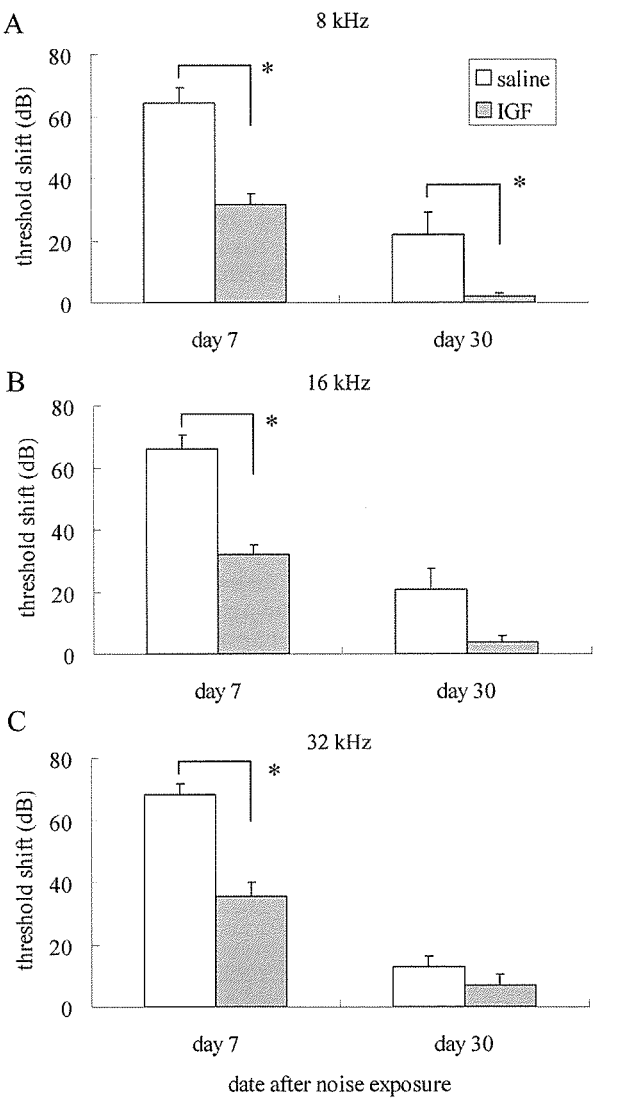

Fig. 1. Auditory brain response threshold shifts for recombinant human insulin-like growth factor-1- (rhIGF-1) and saline-treated cochleae at 8, 16, and 32 kHz on days 7 and 30 after noise exposure. An overall effect of local rhIGF-1 treatment is significant at 8, 16, or 32 kHz (two factorial analysis of variance). Asterisks are indicated significant differences in pairwise comparisons with Fisher's protected least-significant difference. Bars represent standard error (SE).

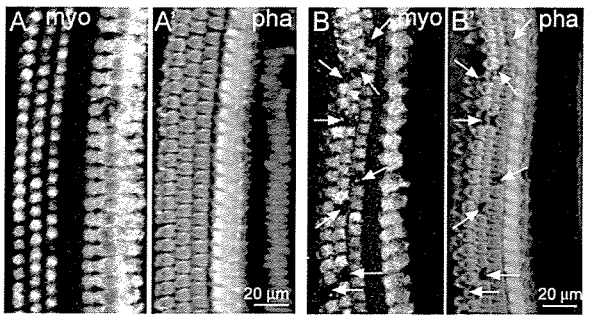

Fig. 2. Photomicrographs of surface preparations stained with myosin VIIa and phalloidin from the second turn of cochleae treated with recombinant human insulin-like growth factor-1 (**A**) or physiological saline (**B**) on day 30. Figures A and B show immunostaining for myosin VIIa (myo), and Figures A' and B' show F-actin labeling by phalloidin. Arrows indicate missing outer hair cells.

at pH 7.4 was gently introduced into the perilymphatic space of the cochleae. The temporal bones were then excised and immersed in the same fixative at 4°C for 12 hours. After rinses with PBS, the cochleae were dissected from the temporal bones and subjected to histologic analysis in whole mounts. We used three regions of cochlear sensory epithelia at a distance of 30% to 40% (apical), 50% to 60% (middle) or 80% to 90% (basal) from the apex for quantitative assessments of hair cell loss.

Immunohistochemistry for myosin VIIa and F-actin labeling by phalloidin were used to label the surviving inner hair cells (IHCs) and outer hair cells (OHCs). Anti-myosin VIIa rabbit polyclonal antibody (1:300; a gift from Tama Hasson, San Diego, CA) was used as the primary antibody, and Alexa-594-conjugated antirabbit goat IgG (1:400; Molecular Probe, Eugene, OR) was used as the secondary antibody. After immunostaining for myosin VIIa, specimens were stained with FITC-conjugated phalloidin (1:300; Molecular Probe). Specimens were viewed using a Leica TCS SP2 confocal microscope (Leica Microsystems Inc., Wetzlar, Germany). Nonspecific labeling was tested by omitting the primary antibody from the staining procedures. We counted the numbers of IHCs and OHCs in 0.2-mm long regions of the apical, middle, or basal portion of cochleae, respectively.

Statistical Analyses

An overall effect on ABR threshold shifts of application of rhIGF-1 was examined by the two-way factorial analysis of variance. When the interaction was significant, multiple comparisons with Fisher's protected least-significant difference (PLSD) were used for pairwise comparisons. The differences in OHC numbers in each region of the cochlea between the rhIGF-1- and saline-treated cochleae were examined using the Student t test. A P value less than .05 was considered statistically significant. Values are expressed as the mean ± standard error.

RESULTS

Functional Protection

The time course of alterations in ABR threshold shifts after noise exposure at 8, 16, or 32 kHz is shown in Figure 1. Local rhIGF-1 treatment demonstrated significant effects on ABR threshold shifts at each frequency. An overall effect on data for 8 kHz of rhIGF-1 application was significant ($P < .001$). The differences in threshold shifts between rhIGF-1- and saline-treated cochleae on days 7 and 30 were significant at multiple comparisons with Fisher's PLSD ($P < .001$ for day 7, $P = .039$ for day 30). An overall effect on data for 16 or 32 kHz of rhIGF-1 application was significant ($P < .001$ for 16 kHz, $P = .005$ for 32 kHz). The difference in threshold shifts at 16 kHz between rhIGF-1- and saline-treated cochleae was significant on day 7 ($P < .001$), but not on day 30 ($P = .051$). The difference in threshold shifts at 32 kHz between rhIGF-1- and saline-treated cochleae was significant on day 7 ($P < .001$), but not on day 30 ($P = .48$).

Histologic Protection

Immunostaining for myosin VIIa and phalloidin staining demonstrated degeneration of OHCs in the apical, middle, and basal portions of saline-treated cochleae (Fig. 2B), whereas OHC degeneration was very limited in rhIGF-1-treated cochleae (Fig. 2A). Conversely, IHC loss was not apparent in every region of both saline- and rhIGF-1-treated cochleae. Quantitative assessments revealed the significant differences in the degree of OHC loss between saline- and rhIGF-1-treated cochleae on days 7 and 30 (Fig. 3). The differences in the degree of OHC loss between the saline- and rhIGF-1-treated cochleae were significant in the apical ($P = .0006$), middle ($P < .0001$), and basal portion ($P = <.0001$) of cochleae on day 7, and in the apical ($P = .0006$), middle ($P < .0001$), and basal portion ($P = .002$) of cochleae on day 30. IHC loss was 2.7 ± 1.3% in the basal, 1.0 ± 0.5% in the middle, or 1.1 ± 0.8 in the apical portion of saline-treated cochleae, and 2.0 ±

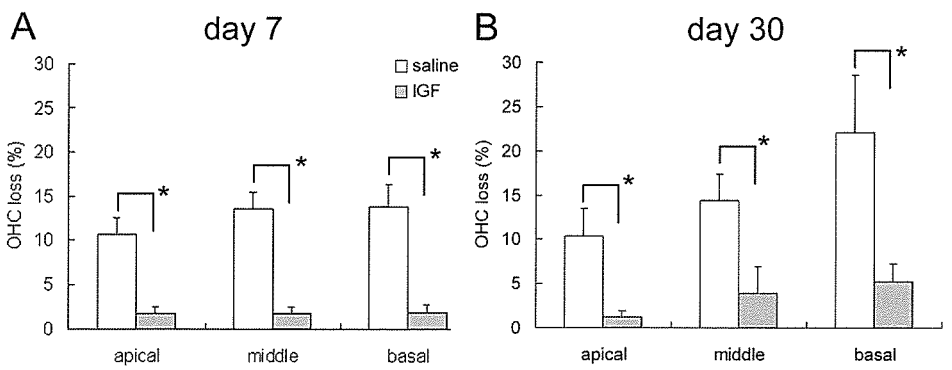

Fig. 3. Means of the percentage outer hair cell loss in the apical, middle, and basal portions of insulin-like growth factor-1- and saline-treated cochleae on days 7 (**A**) and 30 (**B**). Asterisks indicate significant differences with unpaired t test. Bars represent standard error (SE).

1.4% in the basal, 1.2 ± 0.9% in the middle, or 0.6 ± 0.6 in the apical portion of rhIGF-1-treated cochleae on day 30. No significant differences in the loss of IHCs were identified between the two experimental groups.

DISCUSSION

Our findings demonstrate that local rhIGF-1 application using a hydrogel before noise exposure has significant effects on reduction of ABR threshold shifts and of OHC loss. Our previous study has demonstrated the efficacy of local BDNF delivery to the cochlea by the biodegradable hydrogel.[3] The present findings therefore indicate that the biodegradable hydrogel can be used for local rhIGF-1 application to the cochlea. Our previous findings[3] demonstrate that high concentrations of BDNF in the cochlear fluid are maintained during days 3 to 7 after local BDNF application using this system. We then locally applied rhIGF-1 3 days before noise exposure to obtain sufficient concentrations of rhIGF-1 in the cochlear fluid. As expected, the pretreatment with rhIGF-1 demonstrated sufficient protective effects against noise trauma in the present study. However, in clinical settings, drug application after the onset of hearing loss is usually performed. Hence, we should examine the efficacy of local rhIGF-1 treatment after onset of hearing loss in the near future.

In the present study, we focused on degeneration of sensory hair cells in histologic analysis, because the degree of hair cell loss has traditionally been used to evaluate both the extent of noise-induced injury and the efficacy of protective treatments.[9,10] Quantitative assessments in the present study demonstrated significant protection of OHCs from noise trauma by local rhIGF-1 treatment. As for mechanisms of OHC protection by rhIGF-1, several possible explanations are aroused. One possible explanation is the rescue of OHCs from apoptosis resulting from noise by rhIGF-1. IGF-1 is known to inhibit apoptosis by downregulating the expression of proapoptotic genes,[11] and apoptosis is involved in OHC degeneration resulting from noise.[12] Another mechanism is the regulation of glucose transporters in OHCs by rhIGF-1. The expression of glucose transporter-5 (GLUT-5) in OHCs and its importance in their function have been reported.[13,14] GLUTs operate in the first step of glucose utilization by promoting the transport of glucose across the plasma membrane.[15] IGF-1 can regulate the expression of GLUT-5, thereby promoting neuronal cell survival.[16] Such mechanisms might be involved in the rhIGF-1-induced protection of OHCs against noise-induced injury. Further studies are required for elucidation of detailed mechanisms for the rhIGF-1-induced protection of OHCs.

ABR threshold shifts observed on day 7 remarkably recovered on day 30, whereas the damage in the organ of Corti moderately progressed until day 30. This indicates that ABR threshold shifts observed on day 7 may be caused not only by the damage in the organ of Corti, but also by reversible damages in other regions of the cochlea. In addition, the damage in the organ of Corti on day 7, 10% to 14% loss of OHCs and limited loss of IHCs, is not compatible with over 60 dB ABR threshold shifts. Recent studies have indicated involvement of damages in the cochlear lateral wall in noise-induced HL.[17] Local rhIGF-1 treatment significantly reduced ABR threshold shifts on day 7. IGF-1 has also effects on promotion of survival of fibloblasts.[18] Therefore, protective effects of IGF-1 on the fibrocytes in the spiral ligament may be involved in mechanisms for significant reduction of ABR threshold shifts on day 7.

CONCLUSION

This report demonstrates the efficacy of local rhIGF-1 application using a biodegradable hydrogel for the protection of cochleae from noise-induced hearing loss. Because the materials used in the present study are suitable for clinical application, the present findings encourage us to conduct further studies for clinical application of local rhIGF-1 treatment using the biodegradable hydrogel. However, the exact mechanisms by which rhIGF-1 acts in the cochlea are presently unclear and require further research. Furthermore, rhIGF-1 was applied before the onset of noise-induced hearing loss in the present study. The ability of rhIGF-1 to ameliorate cochlear damages when applied locally after the onset of hearing loss should therefore be examined in an experimental model in the near future.

Acknowledgments

The authors thank T. Hasson for providing the antibody for myosin VIIa.

BIBLIOGRAPHY

1. Arnold W, Senn P, Hennig M, et al. Novel slow- and fast-type drug release round-window microimplants for local drug application to the cochlea: an experimental study in guinea pigs. *Audiol Neurotol* 2005;10:53–63.
2. Tamura T, Kita T, Nakagawa T, et al. Drug delivery to the cochlea using PLGA nanoparticles. *Laryngoscope* 2005; 115:2000–2005.
3. Endo T, Nakagawa T, Kita T, et al. A novel strategy for treatment of inner ears using a biodegradable gel. *Laryngoscope* 2005;115:2016–2020.
4. Varela-Nieto I, Morales-Garcia JA, Vigil P, et al. Trophic effects of insulin-like growth factor-I (IGF-I) in the inner ear. *Hear Res* 2004;196:19–25.
5. Linseman DA, Phelps RA, Bouchard RJ, et al. Insulin-like growth factor-I blocks Bcl-2 interacting mediator of cell death (Bim) induction and intrinsic death signaling in cerebellar granule neurons. *J Neurosci* 2002;22: 9287–9297.
6. Staecker H, Van De Water TR. Factors controlling hair-cell regeneration/repair in the inner ear. *Curr Opin Neurobiol* 1998;8:480–487.
7. Malgrange B, Rigo JM, Coucke P, et al. Identification of factors that maintain mammalian outer hair cells in adult organ of Corti explants. *Hear Res* 2002;170:48–58.
8. Iwakura A, Fujita M, Kataoka K, et al. Intramyocardial sustained delivery of basic fibroblast growth factor improves angiogenesis and ventricular function in a rat infarct model. *Heart Vessels* 2003;18:93–99.
9. Keithley EM, Ma CL, Ryan AF, et al. GDNF protects the cochlea against noise damage. *Neuroreport* 1998;9: 2183–2187.
10. Shoji F, Miller AL, Mitchell A, et al. Differential protective effects of neurotrophins in the attenuation of noise-induced hearing loss. *Hear Res* 2000;146:132–142.
11. Linseman DA, Phelps RA, Bouchard RJ, et al. Insulin-like growth factor-I blocks Bcl-2 interacting mediator of cell

death (Bim) induction and intrinsic death signaling in cerebellar granule neurons. *J Neurosci* 2002;22: 9287–9297.
12. Pirvola U, Xing-Qun L, Virkkala J, et al. Rescue of hearing, auditory hair cells, and neurons by CEP-1347/KT7515, an inhibitor of c-Jun N-terminal kinase activation. *J Neurosci* 2000;20:43–50.
13. Nakazawa K, Spicer SS, Schulte BA. Postnatal expression of the facilitated glucose transporter, GLUT 5, in gerbil outer hair cells. *Hear Res* 1995;82:93–99.
14. Belyantseva IA, Adler HJ, Curi R, et al. Expression and localization of prestin and the sugar transporter GLUT-5 during development of electromotility in cochlear outer hair cells. *J Neurosci* 2000;20:RC116.
15. Bell GI, Kayano T, Buse JB, et al. Molecular biology of mammalian glucose transporters. *Diabetes Care* 1990;13: 198–208.
16. Asada T, Takakura S, Ogawa T, et al. Overexpression of glucose transporter protein 5 in sciatic nerve of streptozotocin-induced diabetic rats. *Neurosci Lett* 1998; 252:111–114.
17. Hirose K, Liberman MC. Lateral wall histopathology and endocochlear potential in the noise-damaged mouse cochlea. *J Assoc Res Otolaryngol* 2003;4:339–352.
18. Heron-Milhavet L, Karas M, Goldsmith CM, et al. Insulin-like growth factor-I receptor activation rescues UV-damaged cells through a p38 signaling pathway. *J Biol Chem* 2001;276:18185–18192.

P52A-0002 Distribution of EFP expressing cells in the developing inner ear of pHes1- or pHes5-EGFP transgenic mouse

Ken Kojima, Akiko Sisaoka, Shinji Takebayashi, Junichi Ito
Department of Otolaryngology-Head and Neck Surgery, Graduate School of Medicine, Kyoto University, Japan

Basic helix-loop-helix (bHLH) transcription factors play crucial roles in development of the central and peripheral nervous systems. To visualize expression of Hes1 or Hes5 gene, pHes1- and pHes5-EGFP transgenic (tg) mice were generated (Ohtsuka et al., 2006). In each transgenic mouse, a promoter of Hes1 or Hes5 gene drives enhanced green fluorescent protein (EGFP) gene. In the inner ear, it is suggested that Hes1 or Hes5 regulate cell division and differentiation of sensory and supporting cell progenitors via notch signaling pathway. By use of immunohistochemical technique, we examined distribution of GFP expressing cells in the inner ear of the transgenic mice from embryonic day 10 (E10) to postnatal day 60 (P60). In the pHes1-EGFP tg mouse inner ear, GFP immunoreactive (GFP-IR) cells were observed from E10 to P60. In the pHes5-EGFP tg mouse inner ear, GFP-IR cells were observed from E16.5 to P15. GFP-IR cells in pHes1-GFP tg mouse are candidates of sensory cell progenitors in mature mammalian inner ear.

Reference

Ohtsuka et al., 2006 Mol. Cell Neurosci

P52A-0003 Expression of zfh-5 in the developing mouse brain: mRNA, antisense RNA and protein expression

Toriko Kimura[1], Kenji Sakamuro[2], Motoya Katsuki[2], Tetsuo Yamamori[1]
[1]National Institute for Basic Biology, Okazaki, Japan; [2]Mitsubishi Kagaku Institute of Life Science, Machida, Japan

ZFH-5 is a transcription factor containing three homeodomains and 18 Zn fingers and expressed in differentiating neurons. We have reported that the level of zfh-5 mRNA is negatively regulated by antisense transcripts of the zfh-5 gene. In several types of neurons, including pyramidal cells in the hippocampus and granule cells in the cerebellum, the zfh-5 antisense RNA is expressed prior to the mRNA, as the level of the antisense RNA gradually decreases, zfh-5 mRNA starts to be expressed. Recently, we have raised an antibody against mouse ZFH-5 and examined the expression profile of the ZFH-5 protein. In the most regions of the brain, the protein expression pattern coincided with that of mRNA. However, in the several types neurons mentioned above, ZFH-5 protein was not detected even when the zfh-5 mRNA was already expressed. This observation together with other data suggested that the ZFH-5 gene is level is regulated by several mechanisms including suppression by the antisense RNA and translational control.

P52A-0004 Zic1 and Zic3 synergetically control forebrain development

Takashi Inoue[1], Maya Ota[1], Kazuhiko Mikoshiba[2], Jun Aruga[1]
[1]Laboratory for Comparative Neurogenesis, RIKEN BSI, Saitama, Japan; [2]Laboratory for Developmental Neurobiology, RIKEN BSI, Saitama, Japan

Zic family zinc finger proteins play various roles in animal development. In mice, five Zic genes (Zic1–5) have been reported. Despite their partially overlapping expression profiles, mouse mutants for each Zic gene show distinct phenotypes, suggesting the functional redundancy of Zic proteins. It is expected that the common and specific roles of mouse Zic proteins can be clarified by studying compound mutant mice. In the present study, we characterized Zic1/Zic3 compound mutant mice. Mice carrying homozygous Zic1 mutant allele together with Zic3 null allele showed defects in midline structures, including abnormalities in forebrain and thalamus. Especially, the compound mutants showed severe anatomical abnormalities in the dorsal and ventral telencephalon and olfactory system, which are not obvious in either Zic1- or Zic3-single mutant. These observations indicate that Zic1, in cooperation with Zic3, have an essential role in controlling proliferation and differentiation of the neuronal progenitors in the medial telencephalon.

P52A-0005 Expression of RIP56, a novel zinc finger transcriptional repressor, in developing mouse brain

Chiaki Maruyama, Haruo Okado
Department of Molecular Physiology, Tokyo Metropolitan Institute for Neuroscience, Japan

RIP56, a novel zinc finger protein containing a POZ domain, functions as a sequence specific transcriptional repressor. RIP56 gene disrupted mice show severe abnormalities in brain cortical layer formation, suggesting that RIP56 has a crucial role in cerebral development. To understand the role of this protein in brain development, we examined RIP56 gene expression in mouse embryo and adult brain by in situ hybridization. As a result, we found that RIP56 transcripts are first detected at embryonic day 10 in the neuroepithelium of the spinal cord and telencephalic vesicle. In the day 12–15 embryos, RIP56 transcripts are predominantly observed in the preplate region but not in outside the nervous system. At E15, RIP56 transcripts were detected throughout the neocortex and hippocampus, but not in the thalamus and striatum. In the cortex, the transcripts were detected primarily in cortical neurons, but not in the marginal zones and ventricular zone. In adult mice, RIP56 is expressed in neocortical and hippocampal neurons and granule cells in the cerebellar cortex.

P52A-0006 Lack of NZF-2/MyT1 and NZF-3 transcription factors result in defects of neuronal differentiation and arthrogryposis multiplex congenita

Tsutsui Kameyama, Fumio Matsuzaka, Yuzo Kadowaki, Tohru Matsuzaki
Division of Cell Biology, Fujita Health University, Toyoake, Japan

Neural zinc finger (NZF) proteins are transcription factors with DNA-binding domains of C2HC-type zinc finger motifs. Using P19 cells, we demonstrated that NZFs were expressed transiently during neuronal differentiation, and forced expression of NZF cDNAs resulted in neuronal differentiation. These results suggest that NZF family have a function to regulate neuronal differentiation. To elucidate in vivo functions of NZF family in detail, we generate knockout mice of NZF-2 and NZF-3 respectively. NZF-2 null mice are born alive, but die within 10 min after birth with cyanosis. On the other hand, NZF-3 null mice are viable, fertile and appear normal. These mice look normal morphologically. Then we generate double knockout mice of NZF-2 and NZF-3 by intercrossing. Double knockout mice have a feeding problem and arthrogryposis multiplex congenita. And we find out that the spinal nerves projecting forelimb and trunk are decrease dramatically in the double knockout mice embryo.

Available online at www.sciencedirect.com
SCIENCE DIRECT®
Experimental Neurology 198 (2006) 12–24
Experimental Neurology
www.elsevier.com/locate/yexnr

Cell transplantation to the auditory nerve and cochlear duct

Tetsuji Sekiya [a,*], Ken Kojima [a,b], Masahiro Matsumoto [a], Tae-Soo Kim [a], Tetsuya Tamura [a], Juichi Ito [a]

[a] *Department of Otolaryngology—Head and Neck Surgery, Kyoto University Graduate School of Medicine, Sakyo-ku, Kyoto 606-8507, Japan*
[b] *Establishment of International Center of Excellence (COE) for Integration of Transplantation Therapy and Regenerative Medicine, Kyoto University Graduate School of Medicine, Kyoto 606-8507, Japan*

Received 31 May 2005; revised 22 October 2005; accepted 4 November 2005
Available online 22 December 2005

Abstract

We have developed a technique to deliver cells to the inner ear without injuring the membranes that seal the endolymphatic and perilymphatic chambers. The integrity of these membranes is essential for normal hearing, and the technique should significantly reduce surgical trauma during cell transplantation. Embryonic stem cells transplanted at the internal auditory meatal portion of an atrophic auditory nerve migrated extensively along it. Four–five weeks after transplantation, the cells were found not only throughout the auditory nerve, but also in Rosenthal's canal and the scala media, the most distal portion of the auditory nervous system where the hair cells reside. Migration of the transplanted cells was more extensive following damage to the auditory nerve. In the undamaged nerve, migration was more limited, but the cells showed more signs of neuronal differentiation. This highlights an important balance between tissue damage and the potential for repair.

Keywords: Auditory nerve; Cell migration; Cell transplantation; Embryonic stem cell; Membranous labyrinth; Spiral ganglion cell

Introduction

Cell transplantation provides a potential method to replace the irreversible loss of auditory hair cells and neurons that accompanies many forms of permanent hearing loss. A fundamental requisite is to deliver the potentially restorative cells to the target, usually the site of the lesion, with minimal trauma to the homeostasis of the host. This is particularly difficult in the inner ear because it has a highly specialized and complex anatomy (Fig. 1). Hair cells are an important target for cell replacement, but they occupy a critical position at the boundary between the cochlear chambers that enclose the endolymph and perilymph. The differential ionic composition of these fluids is essential for maintenance of the endocochlear potential that provides the driving force for sound transduction.

Current surgical techniques in the cochlea break the membranes between the chambers, a process that may disturb or, at worst, abolish the residual hearing of the affected patients. This issue applies not only to cell transplantation (Bianchi and Raz, 2004; Brown et al., 1993; Holley, 2002; Ito et al., 2001; Izumikawa et al., 2005; Staecker et al., 2001) (Figs. 1, [1, 1′]–[3]) but also to the inoculation of vectors used for gene transfection (Bianchi and Raz, 2004; Izumikawa et al., 2005) (Fig. 1, [1]). One alternative is to deliver materials into the endolymphatic space through the vestibular aqueduct (Fig. 1, [1′]). However, these procedures may potentially put endolymphatic structures at risk of injury. Another problem with this technique is that the injected materials may enter not only the cochlear but also the vestibular portion of the membranous labyrinth (Fig. 1).

An osmotic pump can be used to deliver various materials such as cells, viral vectors, or pharmacological agents into the perilymphatic space (Brown et al., 1993) (Fig. 1, [2]). Although direct damage to the endolymphatic structures may be attenuated with this technique, this approach may not be totally free from hearing loss due to perilymphatic fluid fistula (Minor, 2003). Another potential danger of one perilymphatic injection technique is that the injected materials could enter the cochlear aqueduct (Fig. 1, CA) and travel through cerebrospinal fluid to the contralateral ear where they could cause unintended effects. More indirectly, the round window niche has been used as the

* Corresponding author. Fax: +81 75 751 7225.
E-mail address: tsekiya@ent.kuhp.kyoto-u.ac.jp (T. Sekiya).

0014-4886/$ - see front matter © 2005 Elsevier Inc. All rights reserved.
doi:10.1016/j.expneurol.2005.11.006

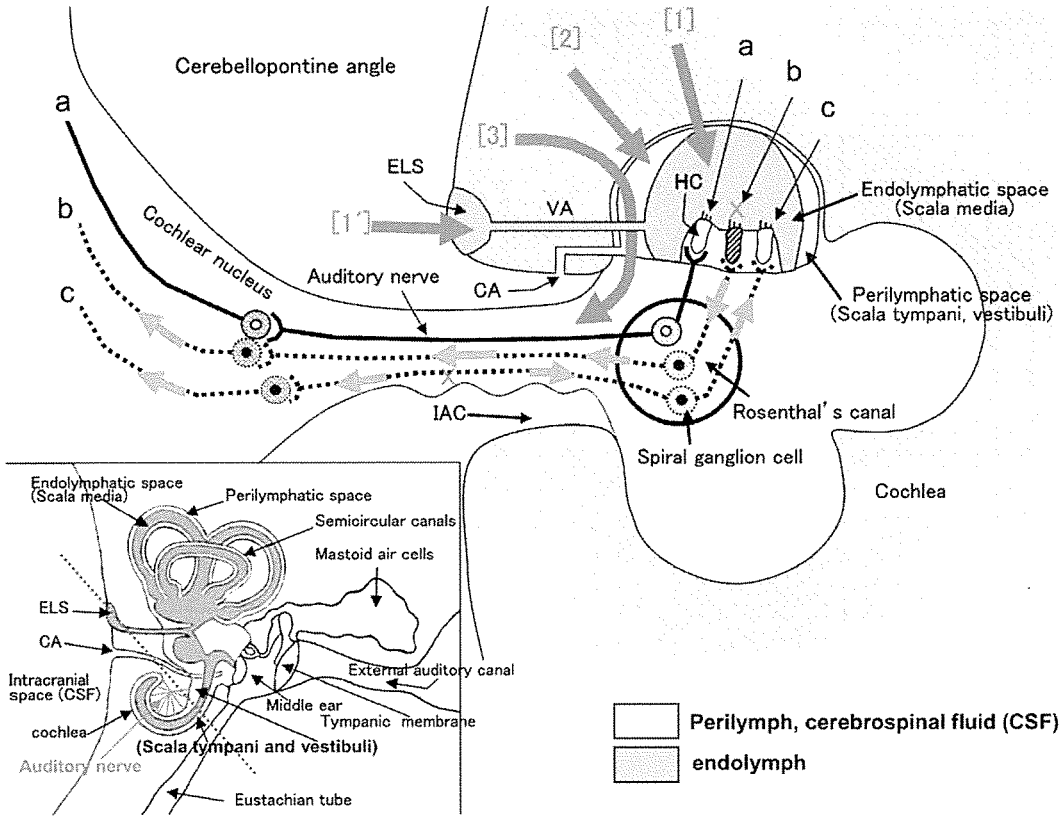

Fig. 1. Schematic representation of normal (a) and pathological (b, c) auditory nerve functional pathways and previously reported approaches ([1], [1′], [2], [3]) to transplanting cells or neuro-regenerative substances into the membranous labyrinth. Normally (a), bipolar auditory neurons synapse with hair cells (HC) distally and with cochlear nucleus cells proximally. When HCs are damaged (b, red x and crosshatched hair cell), degeneration proceeds toward the spiral ganglion neurons and cochlear nucleus cells (b, green arrows). When the auditory nerve is damaged (c) in the CP angle (red x in the middle of the figure), nerve degeneration proceeds bi-directionally as indicated by the green arrows on either side of the x along pathway c. When the membranes enclosing an endo- or perilymphatic fluid-filled space are mechanically breached (interventions [1], [1′], [2], [3]), hearing is compromised. CA, cochlear aqueduct; ELS, endolymphatic sac; IAC, internal auditory canal; VA, vestibular aqueduct. Inset: three-dimensional representation of temporal bone. The blue dotted line indicates the plane of the main figure.

placement site for diffusible materials. However, diffusion of the materials is limited to the more basal turns of the cochlea in this technique, and doses of drugs infiltrating the perilymphatic space are impractical to evaluate. Moreover, non-diffusible materials such as cells cannot be transferred into the membranous labyrinth with this technique.

Transplantation into the modiolus or auditory nerve trunk invades the membranous labyrinth, thus also placing hearing at the risk (Fig. 1, [3]) (Hu et al., 2004a; Regala et al., 2005).

We have developed an effective rat model for cell transplantation in which we have aimed to minimize the damage to cochlear function and potentially to maximize the beneficial outcome. Our method involves transplantation to the internal auditory meatal (IAM) portion of the auditory nerve. To test our model, we transplanted embryonic stem (ES) cells into both damaged and undamaged nerve tissue. We found that transplanted cells migrated along the entire course of the atrophic auditory nerve, even into Rosenthal's canal (RC), where the spiral ganglion cells (auditory ganglion cells) had been located, and finally to the most distal region of the auditory nervous system, the scala media. The fact that cells reached the normal location of the hair cells means that the technique is potentially valuable for replacement of both hair cells and sensory nerves without disrupting the normal balance of endolymph and perilymph. We also found that migration was reduced and neuronal differentiation enhanced in the absence of damage to the nerve. Our technique is based on that refined by the first author over the past 20 years of research in auditory nerve degeneration and regeneration employing more than 5000 experimental animals, including dogs, monkeys, baboons, and, more recently, rats (Sekiya et al., 2000, 2003; Yagihashi et al., 2005).

Materials and methods

Under normal conditions of the auditory nerve and cochlea, spiral ganglion neurons synapse with hair cells distally and with the cochlear nucleus cells proximally (Fig. 1, a). However, various disturbances in nerve transmission can occur and have been described clinically. When the hair cells are damaged, for example, in cases of aminoglycoside ototoxity or sound overstimulation, the spiral ganglion neurons degenerate secondarily (Sekiya et al., 2000; Yagihashi et al., 2005) (Fig. 1, b). Another possible cause is primary pathology in the auditory nerve, such as is seen with auditory neuropathy or with direct surgical trauma during removal of a vestibular schwannoma (Sekiya et al., 2000, 2003; Starr et al., 1996). Under such conditions, the disappearance of spiral ganglion neurons is

caused by retrograde degeneration of the auditory nerve (Fig. 1, c). In both pathological conditions, trans-neuronal degeneration may extend to the cochlear nucleus and upper relay nuclei of the auditory nervous system (Morest et al., 1997) (Figs. 1, b, c). The common element in all of these disorders is degeneration of the spiral ganglion neurons. Therefore, we first reproduced this pathological condition in rats (Sekiya et al., 2000, 2003). In this study, in order to induce direct, rapid, and quantifiable primary degeneration of the auditory nerve, we performed auditory nerve compression in the cerebellopontine (CP) angle of the rat.

Compression of the auditory nerve

All the animal experiments were conducted in accordance with the Guidelines for Animal Experiments at Kyoto University. The auditory nerve of the rats was quantitatively compressed in the CP angle without permanent compromise of the blood supply to the cochlea with the aid of intraoperative monitoring of the compound action potentials of the auditory nerve (CAP) as reported elsewhere (Sekiya et al., 2000, 2003). In the present study, however, we revised the experimental procedures in order to shorten the time during which the labyrinthine artery was transiently compressed. Briefly, male Sprague–Dawley rats weighing 500–550 g each were anesthetized by an intraperitoneal injection of ketamine (100 mg/ml; Sankyo Co., Tokyo, Japan) and xylazine (9 mg/ml; Bayer, Tokyo, Japan). After the rat had been fixed in a small animal stereotactic frame (Model 900, David Kopf Instruments, Tujunga, CA, USA), right suboccipital craniectomy was performed with the aid of a surgical microscope, and the 7th and 8th cranial nerve trunks were identified at the IAM (Sekiya et al., 2000, 2003). An L-shaped stainless steel wire (diameter, 200 μm) was used as the compression-recording (CR) electrode. The CR electrode was placed so that it touched the superior edge of the IAM, and then it was shifted laterally by 7 mm so that its tip touched and remained in contact with the bony surface of the IAM as the electrode was advanced. As the CR electrode was advanced, the auditory nerve was gradually compressed between the tip of the CR electrode and the edge of the IAM (Sekiya et al., 2000). The angle of compression was precisely controlled to apply maximal direct pressure on the nerve with minimal pressure on the artery by having the axis of the electrode tilted posteriorly so the end pointed caudally at an angle of 26.8° from the perpendicular. For the advancement of the CR electrode, a micromanipulator driven by a pulse motor (PC-5N, Narishige, Tokyo, Japan) was used. The operation of this pulse motor was automatically controlled by a programmable controller (Sekiya et al., 2000). As the first compression of the auditory nerve, the CR electrode was advanced at the speed of 1 μm/s until the CAP flattened, termed the "flat point". The CR electrode was maintained at the flat point for 100 s. The rats in which the CAP recovered within 60 s after the flat point was reached, while the CR electrode was maintained at the flat-point position, were included in this study. The depth of electrode advancement for the second compression was 400 μm, and the speed of the electrode advancement was 10 μm/s. Sixty seconds after the start of the second advancement, the electrode was withdrawn at 110 μm/s. In our experimental model, therefore, the auditory nerve and labyrinthine artery were simultaneously compressed during the compression procedure to injure the auditory nerve. However, the duration of complete disappearance of CAPs was less than 60 s in each of two compressions. This amount of CAP loss was far below the critical limit that causes irreversible cochlear ischemia (Pujol et al., 1993; Sekiya et al., 2000).

Electrophysiology

Before the surgical procedures and after the rats were anesthetized, brainstem auditory evoked potentials (BAEPs) were recorded in all rats between the base of the earlobe of the operative side (right) and the vertex with the ground electrode at the base of the forelimb. Click stimuli (90 dB sound pressure level) were presented to the right ear at a rate of 9.5 pulses/s through a tube earphone driven by a 100 μs rectangular pulse wave fed by a stimulator, and evoked potentials were amplified with a bandpass of 50 Hz to 3 kHz and were averaged using a processor (Synax 1100, NEC Medical Systems, Tokyo, Japan) with a sampling interval of 20 μs and 500 data points in each recording. The potentials to 100 successive clicks were averaged and stored in a computer (Sekiya et al., 2000). During the first and second compression procedures, the CAPs were recorded between the tip of the CR electrode and the vertex with the ground electrode placed at the base of the forelimb of the rat. For CAP recordings, the potentials from the nerve to 5 successive clicks were averaged and stored in a computer. This rate led to a continuous CAP recording rate of one potential every 2.4 s before the flat point.

SDIA-treated ES cells

The mouse ES cells that we used, G4-2 (generously donated by Dr. Hitoshi Niwa, Riken Center for Developmental Biology, Kobe, Japan), were a subline derived from E14tg2a ES cells, and they express the enhanced green fluorescent protein (EGFP) gene driven by a ubiquitous strong promoter (CAG promoter) (Kawasaki et al., 2000; Sakamoto et al., 2004). Undifferentiated ES cells were maintained on gelatin-coated dishes in Glasgow minimum essential medium (GMEM) (Invitrogen, Carlsbad, CA, USA) supplemented with 1% fetal calf serum (FCS) (JRH Bioscience, Lenexa, KS, USA), 10% knockout serum replacement (KSR, Invitrogen), 1 mM pyruvate (Sigma, St. Louis, MO, USA), 0.1 mM nonessential amino acids (Invitrogen), 0.2 mM 2-mercaptoethanol (2-ME) (Wako, Osaka, Japan), and 2000 U/ml leukemia inhibitory factor (LIF) (Chemicon, Temecula, CA, USA) for 1 week. Then, the SDIA (stromal-cell-derived inducing activity) method was employed for cell differentiation. Briefly, ES cells were cultured to form differentiated colonies on the PA6 (obtained from RIKEN Cell Bank, RCB1127; a stromal cell line derived from newborn mouse calvaria) feeder layer in GMEM supplemented with 5% KSR, 1 mM pyruvate, 0.1 mM nonessential amino acids, and 0.2 mM 2-ME (differentiation medium) (Kawasaki et al., 2000). The day on which ES cells were seeded on the PA6 feeder layer was defined

as day 0, and, on day 6, ES cell colonies were detached en bloc from the PA6 layer using Collagenase B (Roche Diagnostics, Tokyo, Japan). SDIA-treated ES cells were trypsinized to dissociate into single cells and resuspended in medium at 1×10^5 cells/μl. In the ES cell differentiation method used in the present study, an SDIA promotes neural differentiation of mouse ES cells in vitro before transplantation (Kawasaki et al., 2000).

Transplantation of ES-SDIA cells

Four weeks after compression, we confirmed lack of function of the auditory nerve electrophysiologically by evaluating the results of recordings of BAEPs. Then, the rats were divided into two experimental groups. In the first experimental group (group 1, $n = 9$), we re-anesthetized rats, re-opened the same craniectomy site, and placed enhanced green fluorescent protein (EGFP)-expressing embryonic stem (ES) cells treated with the stromal cell derived inducing activity (SDIA) (labeled ES-SDIA cells) (Kawasaki et al., 2000) at the previously compressed portion (IAM portion) of the auditory nerve. Before placing the cells at the compressed portion of the nerve, we incised the connective tissue capsule of the auditory nerve trunk at the IAM portion in order to facilitate adequate contact between transplanted cells and atrophic auditory nerve fibers. We used utmost caution to avoid additional trauma to atrophic nerve fibers.

In rats in the second experimental group (group 2, $n = 3$), after exposing the auditory nerve as just described, the fused silica tube was inserted into the auditory nerve trunk and then was advanced toward the fundus of the IAC approximately 500 μm. We then infused 5-μl portions of ES cell suspension (1×10^5 cell/μl) in phosphate-buffered saline (PBS), using a microinjector (Micro4, World Precision Instruments, Sarasota, FL, USA), over a period of 5 min.

The external and internal diameters of the fused silica tube for peri-neural transplantation (Group 1) were 170 and 100 μm, while those for intra-auditory nerve transplantation (Group 2) were 107 and 40 μm, respectively.

In both groups of rats, when the tube was in place, we covered the transplantation site with a small piece of absorbable gelatin sponge (Spongel, Yamanouchi, Tokyo, Japan) followed by fibrin glue (Beriplast P, ZLB Behring) to prevent spillage of transplanted cells. No immunosuppressant drugs were employed in the present study.

In order to identify differences in the biological behavior of cells transplanted into normal or atrophic nerve, we transplanted the same volume of the same cells to the IAM portion of an intact auditory nerve ($n = 3$), using the same technique used in group 1 rats.

After the cell transplantation procedure, the rats were kept alive for 4–5 weeks. Then, the animals were killed, and the temporal bones were prepared for histological study.

Another 4 rats were killed 4 weeks after compression without cell transplantation in order to investigate the functional and morphological states of the auditory nerve and cochlea after compression.

Immunohistochemistry

Four to five weeks after cell transplantation, each rat was placed in a state of deep anesthesia and was perfused transaortically with 4% paraformaldehyde in 0.01 M phosphate-buffered saline (PBS) at pH 7.4. Three hours later, both temporal bones and the brain stem were removed en bloc. The tympanic bulla was opened, and the specimen was then immersed in the same fixative for 30 min at 4°C, after which both temporal bones were removed and decalcified with 10% ethylenediaminetetraacetic acid (EDTA) and HCl solution (pH 7.4) for 7 days at 4°C. Serial 5 μm frozen sections of each temporal bone embedded in OCT compound (Sakura Finetechnical, Tokyo, Japan) were made. Among the slices made from these procedures, the section that simultaneously included all four RCs (basal, lower middle, upper middle, and apical) as large as possible and the cochlear nerve with widest width possible was selected as midmodiolar sections. The midmodiolar sections were mounted on glass slides, washed in PBS, and dried in room temperature (RT) air for 30 min. The sections were permeabilized and blocked by 10% goat serum in 0.2% Triton X-100 (Sigma) in PBS at RT for 30 min. A primary antibody (anti-EGFP rabbit serum, ×500; Molecular Probes, Tokyo, Japan, diluted by 10% goat serum in 0.2% Triton X-100 PBS) was applied to the sections and incubated at 4°C for 12 h followed by washing in 0.2% Triton X-100 PBS 2 times for 5 min each. A secondary antibody (Alexa Fluor 594 labeled anti-rabbit IgG goat antibody ×500, Molecular Probes, diluted by 10% goat serum in 0.2% Triton X-100 PBS) was applied to the sections at 4°C for 6 h followed by washing in 0.2% Triton X-100/PBS 2 times for 5 min each. For nuclear staining, the sections were incubated in 4′-diamidino-2-phenylindole (DAPI) (0.1 μg/ml, Roche Molecular Biochemicals, Tokyo, Japan) solution at RT for 30 min. In several sections, nucleic acid dye (TOTO3, ×500, Molecular Probes) was applied for 15 min to stain nuclei for confocal microscopy. They were washed in 0.2% Triton/PBS 2 times for 5 min each. The sections were pre-equilibrated in the SlowFade Equilibration Buffer (Molecular Probes) for 30 min and mounted in SlowFade antifade reagent (Molecular Probes). In several rats, anti-βIII-tubulin rabbit polyclonal antibody (×300; Covance Research Product, Berkeley, CA, USA) was used as the primary antibody to visualize neurites. In each case, the non-operated sides of the cochlea and auditory nerve were used as the control. A fluorescence microscope system equipped with appropriate filters (Olympus BX50 + BX-FLA, Olympus, Tokyo, Japan) was used for observation. Samples were photographed with a digital camera (Olympus DP10). For confocal microscopy, a Leica TCS SP2 confocal laser-scanning microscope (Leica Microsystems, Tokyo, Japan) was used. Images used for the figures were processed with Photoshop and Illustrator software programs (Adobe Systems, Mountain View, CA).

We also performed immunohistochemistry to convert the EGFP into the horseradish peroxidase (HRP) reaction to reconfirm the presence of transplanted EGFP-labeled cells in selected cases. After inactivating endogenous peroxidase with 3% hydrogen peroxide, the sections were permeabilized with